THE UNIVERSITY OF MICHIGAN

College of Engineering

Department of Mechanical Engineering

Cavitation and Multiphase Flow Laboratory

Report No. UMICH 013570-17-T

CAVITATION NUCLEI SIZE DISTRIBUTION IN HIGH-SPEED WATER TUNNEL UNDER CAVITATING AND NON-CAVITATING CONDITIONS

by

O. Ahmed*

F. G. Hammitt**

Financial Support Provided by:

National Science Foundation
Grant No. GK-1889

*Doctoral Candidate, Dept. of Mech. Engr., College of Engr., Univ. of Mich., Ann Arbor, Michigan.

**Professor-in-Charge

April 1972

ABSTRACT

Gas nuclei spectra measurements obtained with our modified Coulter Counter system in cavitating and non-cavitating conditions in our High Speed Water Tunnel are reported. These show the strong dimunition with time of nuclei population during runs of several days, presumably as the gas is continually forced into solution. Total gas content during these runs is held approximately constant. The general shape of the spectra curves then remains approximately constant with time, although strongly diminishing in amplitude. It can be predicted by a quasi-theoretical expression which does not include any empirical constants. Hence its applicability to tunnel flows may be quite general.

The effect of cavitation at the same tunnel velocity is to reduce nuclei content more rapidly than in its absence, even though mean tunnel pressure is less in the cavitating case.

LIST OF FIGURES

Figure		Page
1	Pressure tap locations and water loop installation geometry for 3/4" plexiglas venturi	11
2	Schematic showing Coulter-Counter connection into water tunnel	12
3	Schematic of Coulter-Counter arrangement	13
4	Schematic of water cavitation facility (only two of the four loops are shown)	14
5	Pressure profile for no-cavitation runs	15
6	Run no. 1, no cavitation	16
7	Run no. 2, no cavitation	17
8	Run no. 3, no cavitation	18
9	Run no. 4, no cavitation	19
10	Run no. 5, no cavitation	20
11	Run no. 6, no cavitation	21
12	Run no. 7, no cavitation	22
13	Run no. 8, no cavitation	23
14	Run no. 9, no cavitation	24
15	Run no. 10, no cavitation	25
16	Run no. 1 through no. 10, no cavitation calculated curves of nuclei distribution change with time	26
17	Trial run no. 1, no cavitation calculated spectra	27
18	Trial run no. 2, no cavitation calculated spectra	28
19	Pressure profile for the cavitation runs	29
20	Cavitation, run no. 1,2-loops	30
21	Cavitation, run no. 2, 2-loops	31
22	Cavitation, run no. 3, 2-loops	32
23	Cavitation, run no. 4, 2-loops	33
24	Cavitation, run no. 5, 2-loops	34
25	Cavitation, run no. 6, 2-loops	35
26	Cavitation, run no. 7, 2-loops	36
27	Cavitation, run no. 8, 2-loops	37

(List of figures continued)

Figure		Page
28	Cavitation, run no. 9, 2-loops	38
29	Cavitation, run no. 10	39
3 30	Cavitation, run no. 11	40
31	Cavitation, runs no. 1 through no. 11, 2-loops	41
32	Run no. 1, cavitation, 1-loop	42
33	Run no. 2, cavitation, 1-loop	43
34	Run no. 3, cavitation, 1-loop	44
35	Run no. 4, cavitation, 1-loop	45
36	Run no. 5, cavitation, 1-loop	46
37	Run no. 6, cavitation, 1-loop	47
38	Run no. 7, cavitation, 1-loop	48
39	Run no. 8, cavitation, 1-loop	49
40	Run no. 9, cavitation, 1-loop	50
41	Run no. 10, cavitation, 1-loop	51
42	Run no. 11, cavitation, 1-loop	52
43	Run no. 12, cavitation, 1-loop	53
44	Run no. 13, cavitation, 1-loop	54
45	Run no. 14, cavitation, 1-loop	55
46	Run no. 15, cavitation, 1-loop	56
47	Cavitation runs no. 1 through no. 15, 1-loop	57
48	Entrained gas volume, normalized	58

I Introduction

In a previous technical report (1), a new technique for the measurement of cavitation nuclei concentration and size distribution, was presented. The report had dealt mainly with the explanation of the equipment and instruments used. Also, some preliminary measurements were presented.

In the present report more detailed measurements are made to study the nuclei population in the water tunnel test facility under different conditions.

II Report Objectives

This report will present the results of nuclei population measurements made using the modified Coulter Counter technique. The measurements were made with our "High-Speed Water Tunnel" under non-cavitating and cavitating conditions. Also, the measurements were made on a long-term-run basis with specific attention given to studying the population dependence on pressurization history; i.e., population versus time under constant pressure, velocity, temperature and total air content.

III Experimental Results

A. Nuclei population measurements with the loop under non-cavitation condition

Our "High-Speed Water Tunnel" with two loops running in parallel was filled with tap water (Ref. 1 describes the tunnel). One of the loops, includes the main test section, which is a 3/4" throat diameter venturi without pressure taps. A second loop (in parallel with the first) contains a geometrically identical venturi with wall pressure taps for minitoring the axial pressure profile (fig. 1).

The sampling line for withdrawing water from the loop is connected at the inlet of the test section venturi. It is actually a by-pass line around the venturi to its exit tap. From this line, a small sample line is run into

the modified Coulter Counter for measuring the nuclei population. The arrangement is shown schematically in Fig. 2 and 3.
Fig. 4 is a schematic of the water tunnel into which it is installed.
The gas nuclei measurement is made at approximately tunnel pressure, i.e., the pressure at that position in the tunnel where the sampling probe is located. The Coulter Counter system is essentially isobaric in that frictional losses in its tubing are negligible, since the flow-rate is extremely small, as is the pressure drop through the measuring orifice, compared to the absolute tunnel pressure. Thus there is no significant change in nuclei size due to changing liquid pressure during passage through the instrument from the tunnel conditions. This is true because it is the pressure ratios which are the important parameters for gas bubble growth or collapse in conditions where vapor pressure is low as it is with the cold tunnel water. It is of course necessary to provide an isokinetic sampling probe to obtain a true sample of entrained gas and liquid mixture from the tunnel stream..

To check reproducibility, two relatively short runs were made each for five days. This data will verify the initial behavior of the bubble population which is the fastest changing portion in the history of the population. A final run, which is the main run of this test, lasted for ten days. In all three cases, the nuclei measurements were done at approximately 24 hour intervals. Also, in all three cases, the velocity, temperature, total air content and pressure were maintained constant.

The pressure and velocity were very close to the minimum conditions for the tunnel, i.e., the minimum rpm of the pump and the minimum pressure that will eliminate any cavitation in both venturies. The velocity in the throat was 65 fps, and the corresponding minimum pressure at the inlet to the test section was 44.0 psia. The pressure profile along the axis of the venturi is shown in Fig. 5.

The pressure in the pressure chamber which houses the modified Coulter Counter was kept at 43.6 psia in order to allow for the sample flow into the measuring beaker. The average total gas content measured

by the Van Slyke was 2.75% at atmospheric pressure 14.33 psia and room temperature 65°F.

Since these measurements were going to be done for long term periods, the measuring time was also larger than the case of short period runs done before (1). This is to insure better statistical results specifically by the end of the runs where the density of nuclei in water is expected to decrease substantially. The sample measured in these runs were 100 cc. each time. As it was mentioned before, the interval between measurements was approximately 24 hours. The initial reading was taken about 30 minutes after filling the loop, which is approximately the time needed to adjust the loop parameters and conditions and record the initial conditions readings.

B. Results of the Non-Cavitating Runs

The actual measured population spectra are shown in Fig. 6 through 15. The data points shown in dots are the actual output spectra from the multi-channel-analyzer. Tha absissa of each curve represents the volume of the nuclei in cubic microns. The ordinate represents the number of nuclei corresponding to each nucleus volume per liter of water of the tunnel.

The curves through the experimental data points are as calculated for a least mean square fit of the data about a quasi-theoretical relation derived as explained in the next section. A computer program was written for its use. Figures 16, 17 and 18 present the calculated curves for the three cases run which show the relative change of the nuclei spectrum.

The initial spectra for each run are not exactly the same, since for each run, a new fresh tap water sample was used, and although the initial condition of the tunnel was kept the same, the conditions of the main water line in the building cannot be the same. Consequently the pressurization history of the water in that line are not the same, and in fact this parameter is not under the control of the authors.

The summation of the data points of Fig. 6 through 15, $\sum N(v) v$, represents the total entrained gas content* in the water volume measured sample. Now for the sake of comparison of the three cases to check the reproducibility of the measurements as well as to study the pressure history of the total entrained gas content, the normalized values of $\sum N(v) v$, are plotted versus time and shown in figure 48. From these curves, the total entrained gas content is shown to be falling rapidly in the first few days of the run for the three cases, which appear very similar to each other, indicating good reproducibility of the measurements. The longest duration run in these tests, i.e., the last, is apparently reaching a stabilized nuclei spectrum after the first rapid decrease. The shape of the curve of population with time beyond the last experimental point is presumably asymptotic.

C. Quasi-Theoretical Nuclei Spectra Relation

A quasi-theoretical relationship to be used for the basis of a least-mean square fit to the data, was derived by assuming that the gas exists initially in a single hypothetical large bubble that breaks into small minute different-sized bubbles o "nuclei". From the measured data, the volume of such a single big bubble containing all the gas would be:

$$V = \sum_{v} N(v)\, v$$

where v = volume of given nuclei

N(c) = number of nuclei of volume v

*Assuming solid particle content to be only a small portion of the total, which we believe to be the case, because of the strong dimunition of particle population with time. It appears that only the gas aprticle content would be affected by run duration.

Now for small nuclei of volume v to be formed and to be stable, the pressure inside these bubbles must overcome both the effect of the surface tension and the work done against the ambient outside pressure, i.e., the total work is

$$w(v) = 4\pi r^2\sigma + 4/3\,\pi r^3 p = 4.838\,\sigma v^{2/3} + pv$$

σ = surface tension of water.

The total work stored in all the measured nuclei is

$$W = \sum N(v)w(v) = \sum N(v)\,(4.838\,\sigma v^{2/3} + pv)$$

or

$$W = 4.838\,\sigma\sum N(v)\,v^{2/3} + p\sum N(v)v.$$

the first term (i.e., surface tension term) is very small compared to the second and can be neglected. Therefore:

$$W = p\sum N(v)v = pV$$

This energy is assumed to be divided among the many small individual nuclei. Therefore the actual size distribution, the number of any volume v will be

$$N(v) = \frac{W}{w}$$

We have found that the statistical distribution of the data obtained is proportional to $1/v$. Thus the final best-fit formula is

$$N(v) = \frac{W}{w} \cdot \frac{A}{v}$$

or

$$N(v) = \frac{p\sum N(v)v}{4.838\,\sigma v^{2/3} + pv} \cdot \frac{A}{v}$$

Finally, A has been found to have dependence on the total air contents ratio, i.e. the ratio between the actual air content and the saturated air content at the given pressure of

$$A = \frac{V_{act}}{V_{sat}} .$$

Somewhat surprisingly the above quasi-theoretical formulation describes the shape of the spectra curves without any empirical correction. Thus it may be that this expression is quite general in its applicability to turbulent streams which include entrained gas nuclei. This can only be demonstrated by making similar measurements in an entirely different tunnel using identical instrumentation. It is hoped that this can be eventually done.

D. Nuclei Population Measurements with the Tunnel under Cavitating Conditions

1) Loop Flow Conditions

For these measurements, the loop conditions were adjusted to induce cavitation but for inlet pressure to the test venturi (i.e., the location from which samples are extracted for measurement of nuclei spectra) the same as in the previous cases, so that the nuclei spectra would not be changed by differences in loop pressure. Cavitation was induced by simultaneously increasing the velocity of the flow and reducing the downstream pressure (which would otherwise increase with the velocity increase in the tunnel). The cavitation cloud was adjusted to 3/4" length. This length was chosen more or less arbitrarily since it gave an apparently stable, non-oscillating cavitation cloud throughout the test. The velocity in the venturi throat was 75 fps.

The pressure profile at the final stage of stable loop conditions is shown in figure 19. The nuclei spectra measurements were done following the previous cases.

2) Results of the Cavitating Runs

The results of these measurements are presented here in the same form as already described. The measured population spectra are shown

in Fig. 20 through 30. The parameters for the absissa and ordinates are the same as before.

The same quasi-empirical formula was applied to these measurements and the resulting calculated best fit curves are shown through the experimental data points. Fig. 31, presents the calculated curves for the experimental spectra simultaneously to show the change in these spectra with pressurization history.

The summation of the experimental data $\sum_{v} N(v)\, v$, the total entrained gas content versus time, is shown in figure 48. The data for this curve are scattered and appear to be oscillating. The reason for this oscillation appears to be air leakage from the pressure taps of one of the venturis. A very small air leakage into the tunnel was observed at the minimum pressure tap of this venturi on several occasions. Efforts were made to remedy the situation, but were not completely successful. It was difficult to notice any effect of this leakage on the results from the teletype output of the multi-channel analyzer before the integrated values (done by the computer) were available. Hence the test was continued after the leakage was noticed. In spite of these oscillations in the entrained gas content, the general trend of the curve is as expected, i.e. decreasing with time.

The total gas content measured by Van Slyke was found to increase slightly throughout the test verifying the supposed leakage.

E. Nuclei Population Measurements with the Tunnel under Cavitating Conditions and with Single Loop Only

In order to verify the results of the above measurements, the same measurements were repeated under the same cavitation condition, but with the pressure profile venturi loop disconnected*, i.e., the tunnel containing the test venturi loop only.

* These two loops are normally operated in parallel. See Ref. (1) for general discription of tunnel.

The results of these measurements are shown in figure 32 through 46. These figures present the experimental nuclei population spectra showing the best fit curves calculated as previously explained. Figure 47 shows the simultaneously calculated curves varying with pressurization history. Figure 48 shows the normalized volume of the entrained gas content of these results. With the pressure tap venturi eliminated, no air leaks are possible and it is noted that the nuclei population falls smoothly with time as for the non-cavitating test.

To allow comparison between the cavitating and non-cavitating condition, the normalized curves for both cases are shown in figure 48. The curve for the cavitating condition is noticed to be dropping faster than that for the non-cavitating condition and reaches an asymptotic condition more rapidly. It could be speculated that with a further large increase in test duration both curves will reach the same asymptotic value.

At this point it is not clear why the nuclei population drops more rapidly with cavitation than without. (Tunnel velocity is not the same, but mean tunnel pressure is less for the case with cavitation.) A complete answer has not been reached from the present investigation. However, the following possible explanations can be hypothesized.

Starting with large numbers of both small and large nuclei in the tunnel, cavitation will cause these nuclei to expand as they pass through the low pressure region in the throat and then collapse as they pass on to the high pressure region of the diffuser. This mechanism will cause these original nuclei to disintegrate into smaller nuclei, and the smaller the nuclei, the more probable that they will be dissolved.

Whether it is a case of an organic-skin coated nucleus model, or that of gas entrapped in crevices in solid particles (to cite the two models for nuclei stability usually considered), the present tests suggest that mechanical disintegration of the nuclei will force more of the entrained air into solution. In fact this observation appears more appropriate for the

organic-skin model; however, it is also possible for the other model.

The similarity of the asymptotic behaviour of the cavitating and non-cavitating tests suggest that a minimum amount of entrained gas (in one form or another) is sufficient to sustain a stable cavitation condition. The physical appearance of the cavitation cloud as well as its audible sound, was noticed to change with time, even though pressures, velocities and total gas content remained constant. The length of the cloud decreased slightly and the mean size of bubbles also decreased as observed by strobe light illumination. The audible sound level and frequency were observed to increase, especially when the start of the runs is compared with the end.

IV CONCLUSION

The results of the above measurements suggest that our modified Coulter-Counter technique for the measurement gas nuclei spectra is valid and promising especially for continuous monitoring in water tunnels. With more sophisticated electronic circuitry, direct and continuous read-out could be obtained. The results also show that a relatively small nuclei population is sufficient to sustain a stable cavitation field under suitable pressure and velocity conditions. In fact there is only a slight change in the behavior of a developed cavitation field for an order of magnitude reduction in nuclei population. The results also show that the entrained gas volume is typically only an extremely small fraction of the total gas content, i.e., entrained and dissolved. The ratio is of the order of 10^{-6}.

ACKNOWLEDGEMENTS

The authors would like to acknowledge the assistance of Mr. K.F. Subhani of the Electrical Engineering Department of Wayne State University in writing the computer program for the empirical formula calculations.

Financial support was provided by NSF Grant 1889.

REFERENCES

1. Ahmed, O., Bhatt, N.R. and Hammitt, F.G., "Preliminary Coulter-Counter Measurements in High Speed Cavitation Tunnel", available as ORA UMICH 01357-17-T, University of Michigan, June 1970.

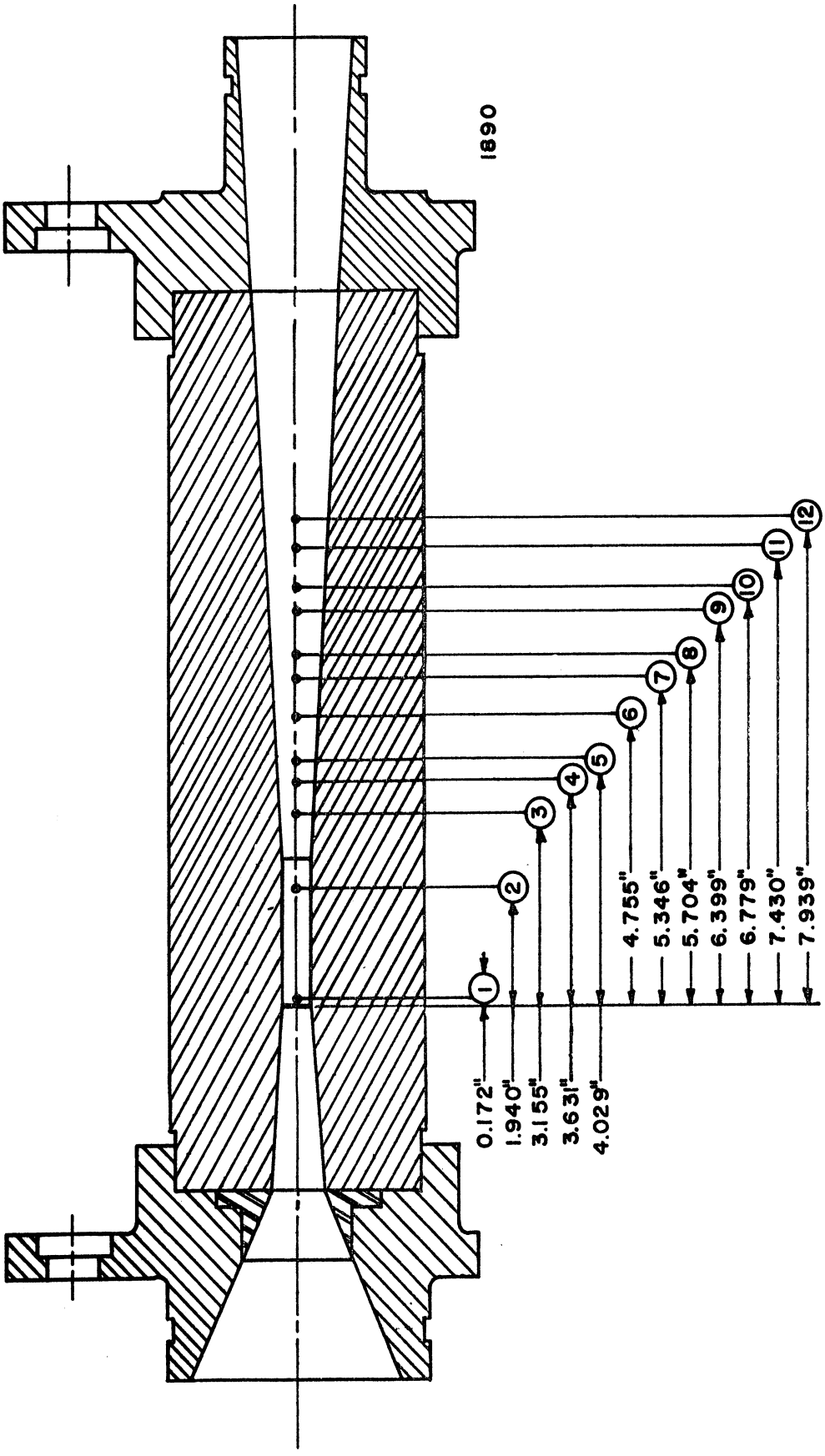

Fig. 1.--Pressure tap locations and water loop installation geometry for 3/4" plexiglas venturi.

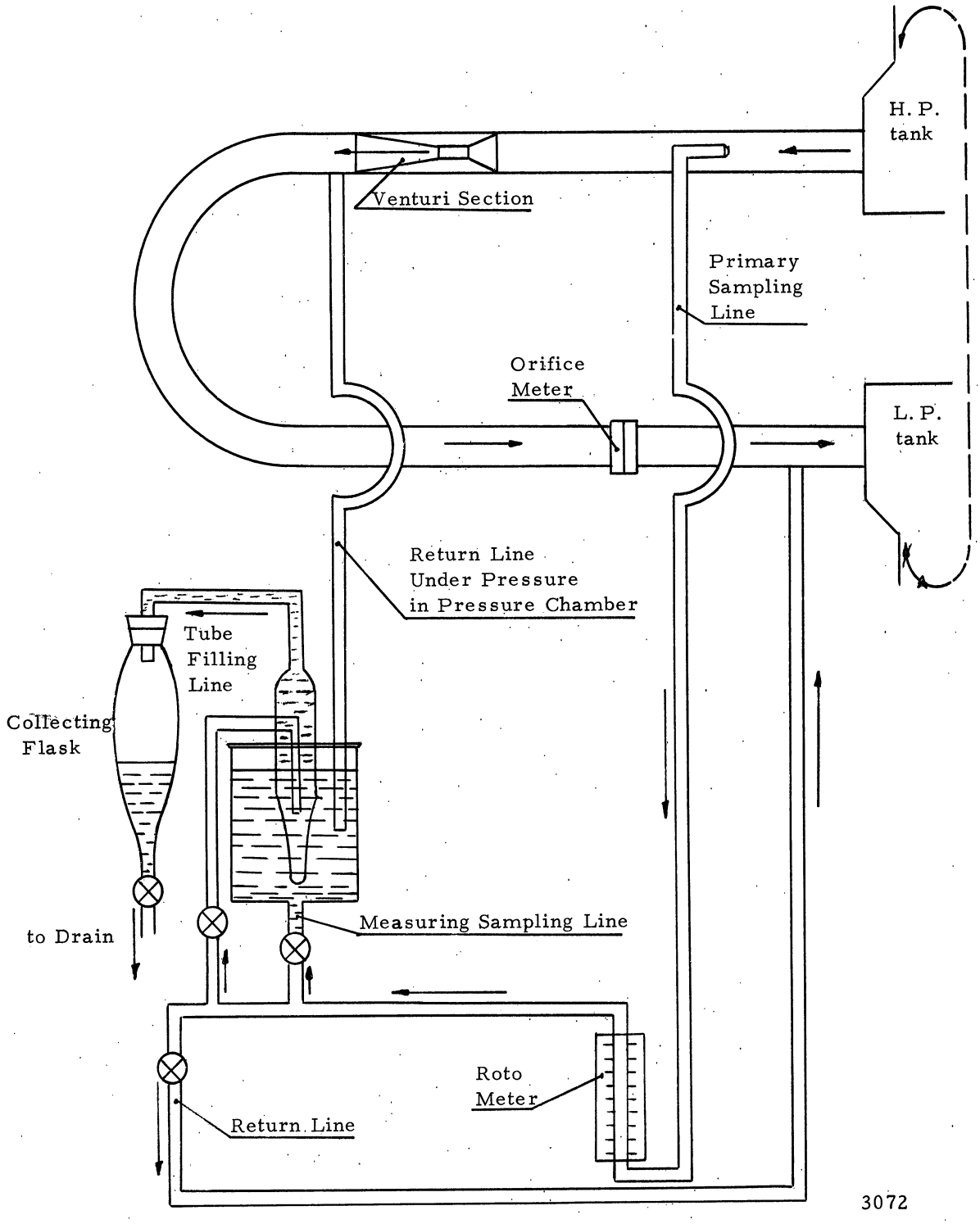

Fig. 2 Schematic showing Coulter-Counter connection into water tunnel

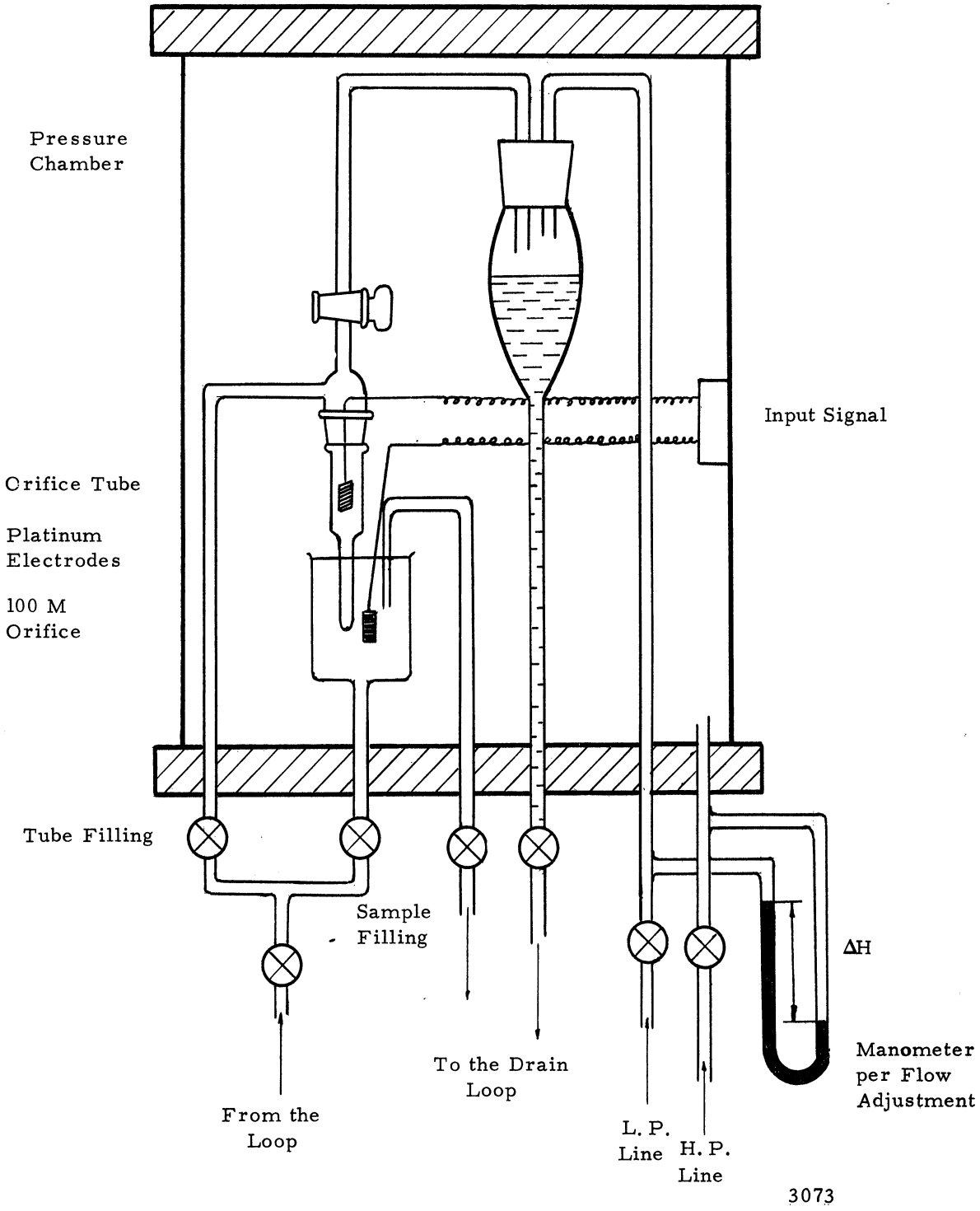

Fig. 3 Schematic of Coulter-Coulter arrangement

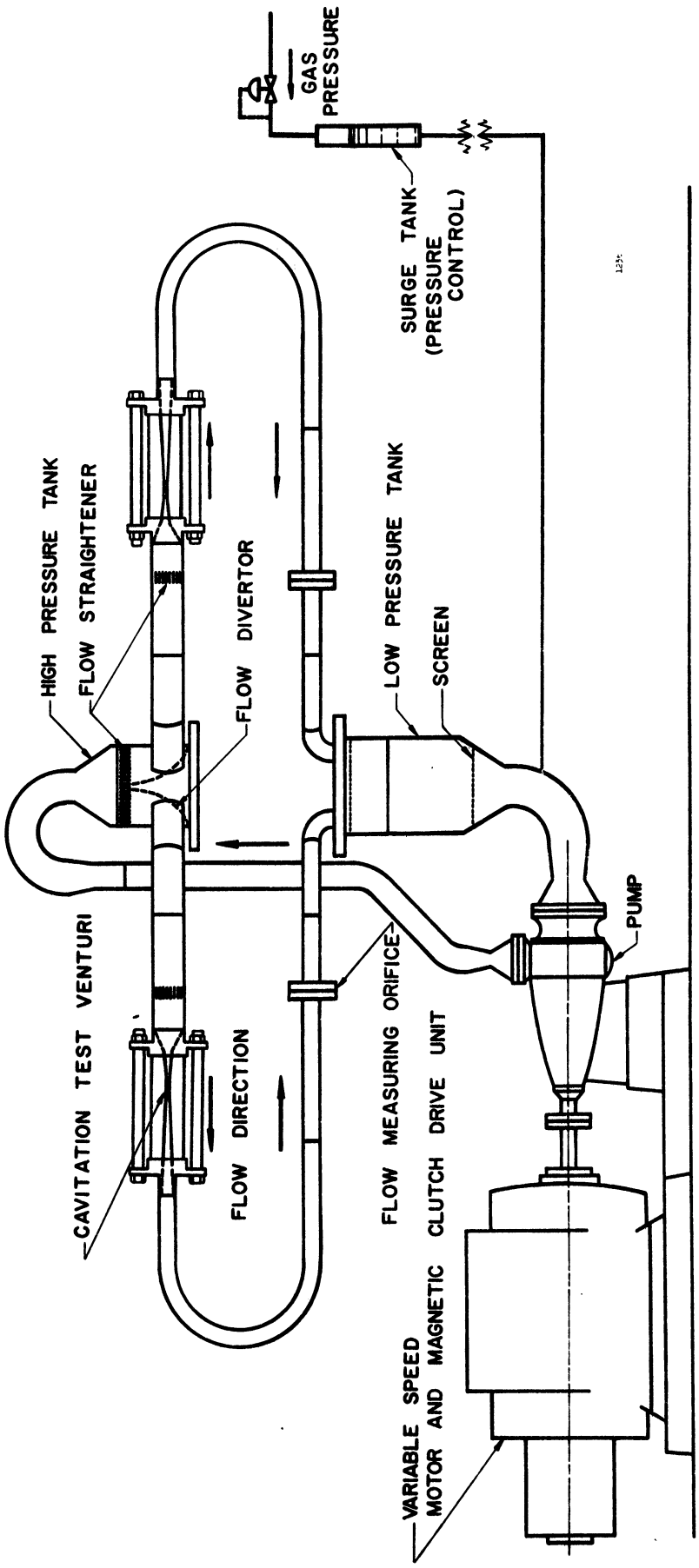

Fig. 4.--Schematic of water cavitation facility (only two of the four loops are shown).

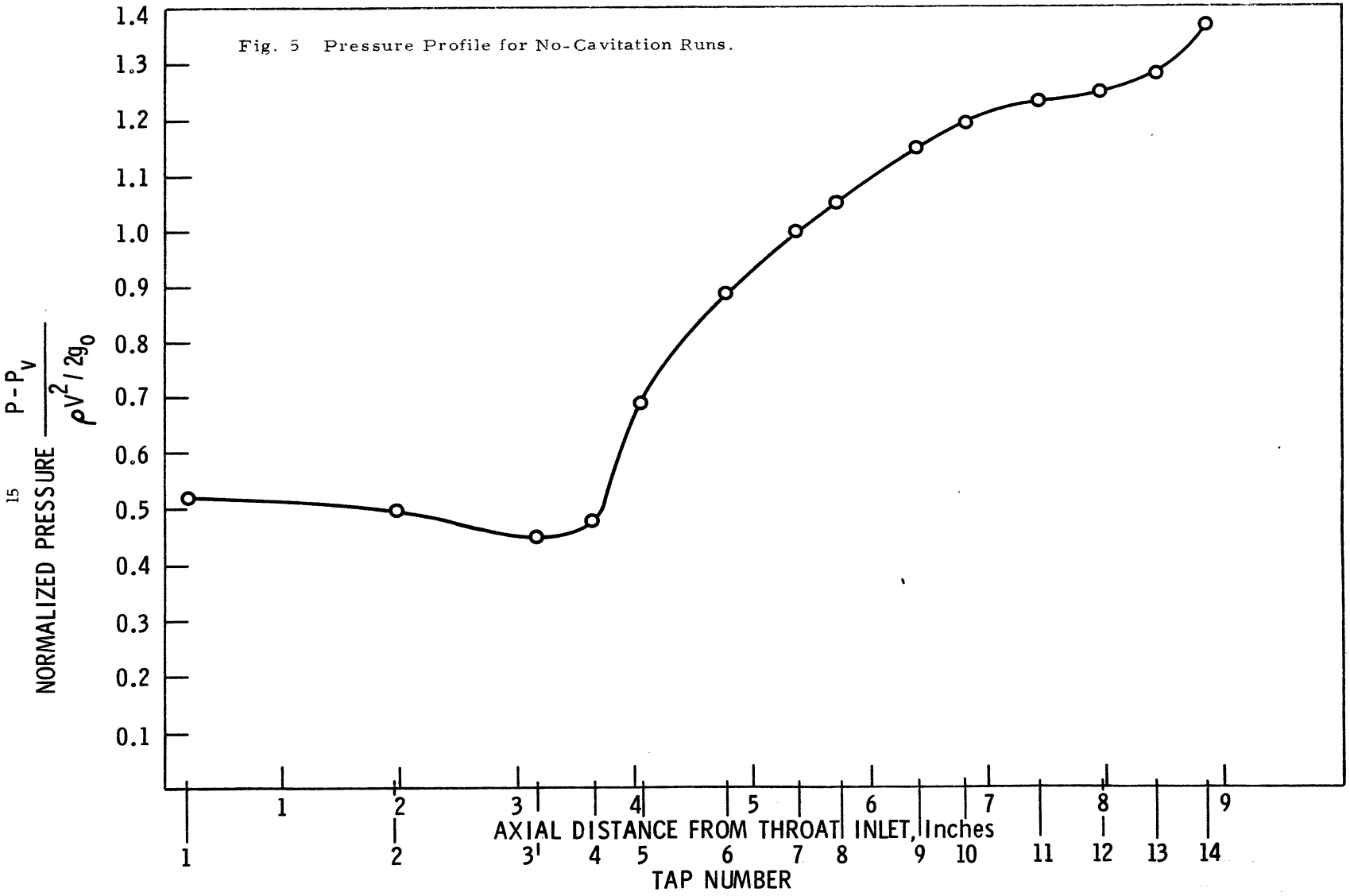

Fig. 5 Pressure Profile for No-Cavitation Runs.

Fig. 6. Run No. 1, No Cavitation

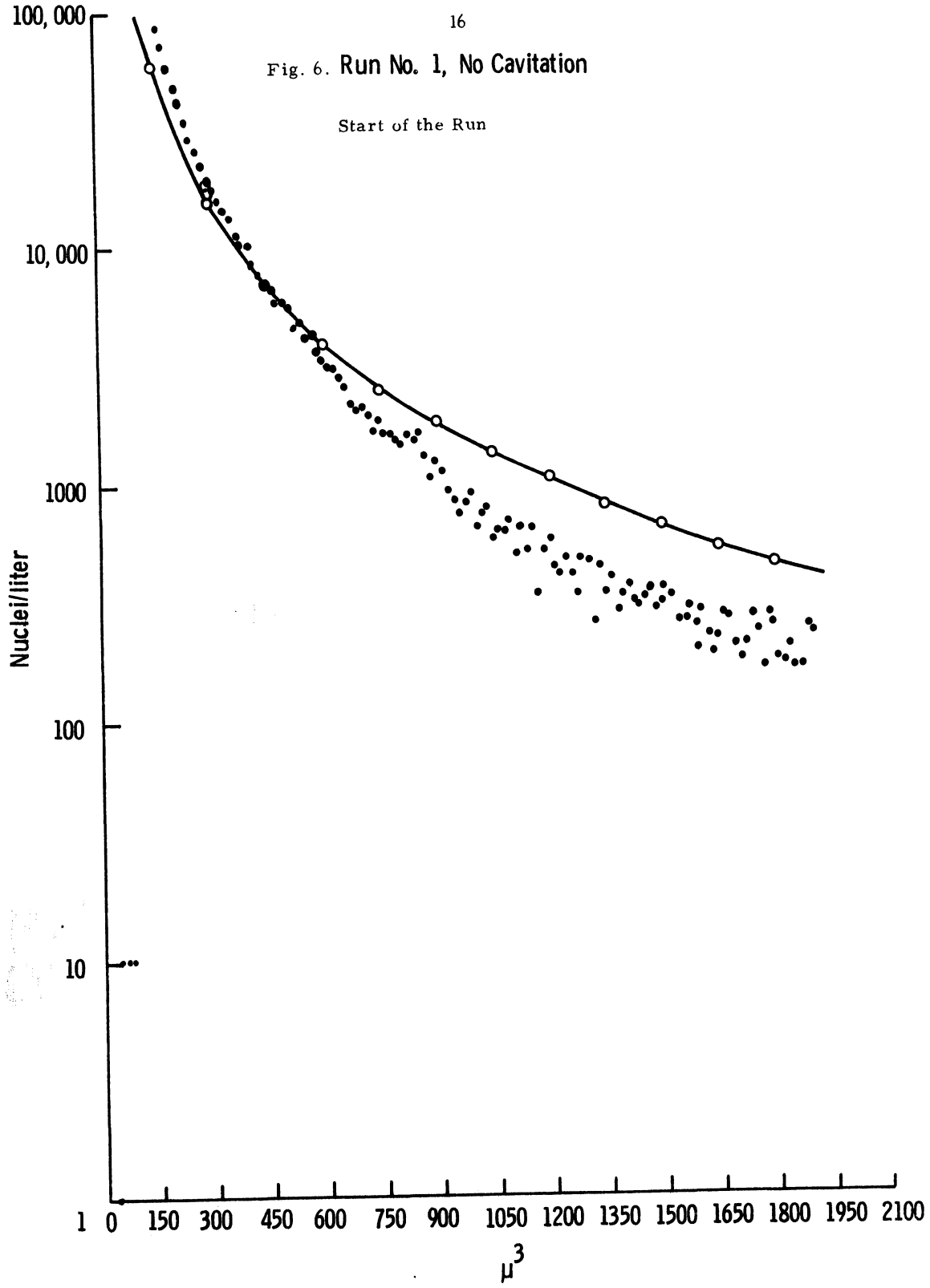

Fig. 7. **Run No. 2, No Cavitation**
23.25 hr. after the start of the run

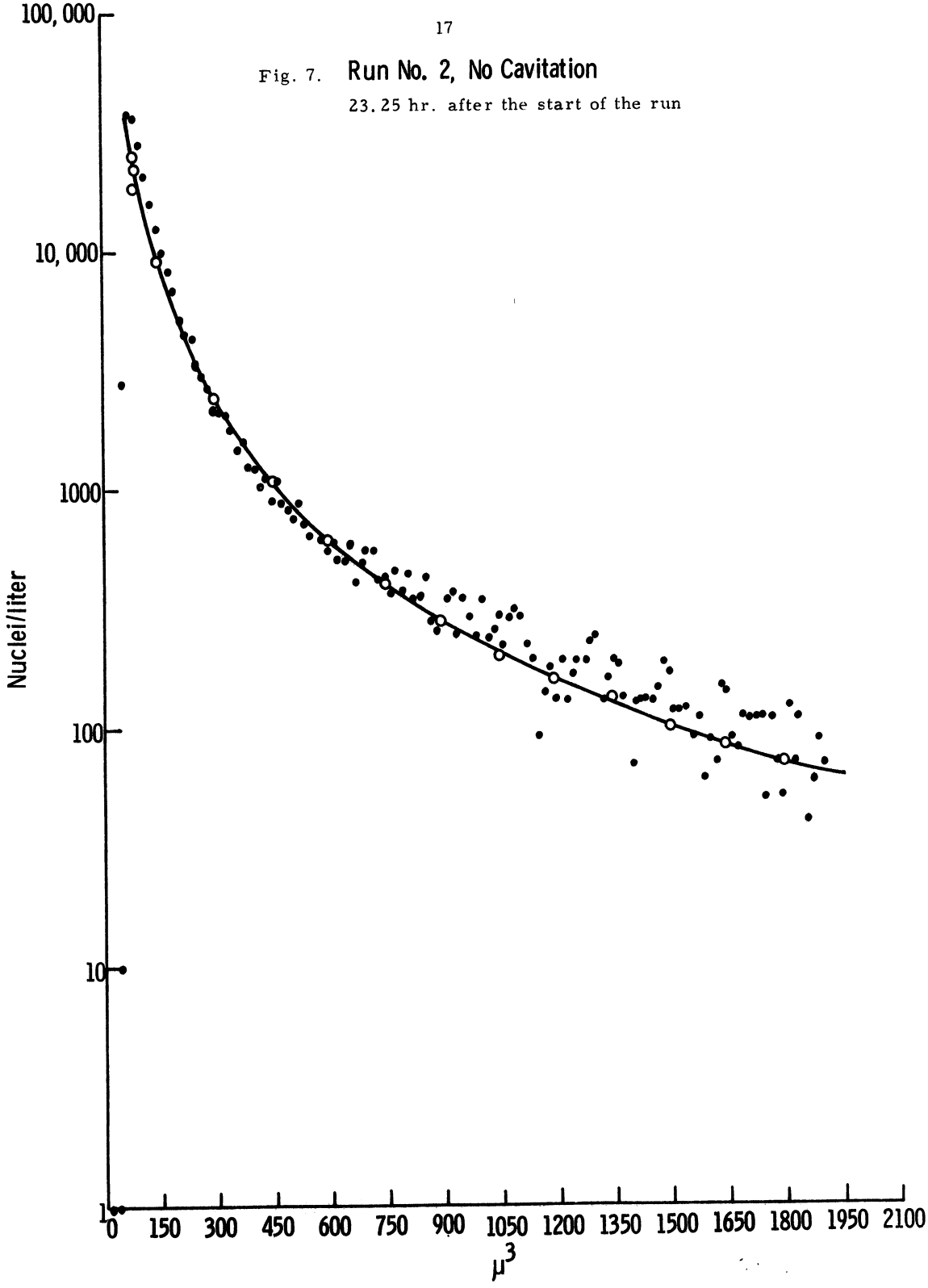

Fig. 8 **Run No. 3, No Cavitation**

46.08 hr. after the start of the run

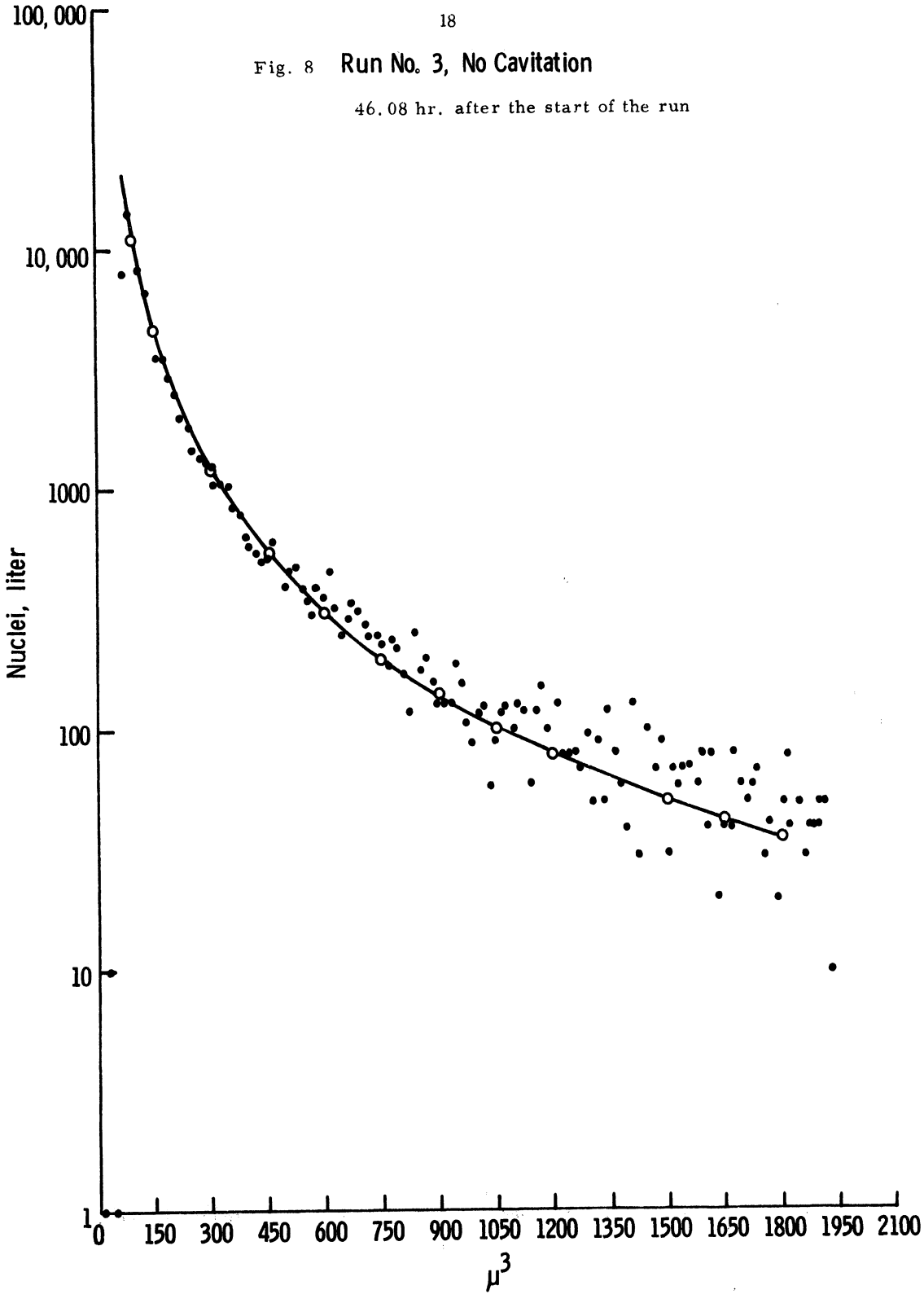

Fig. 9. **Run No. 4, No Cavitation**

71 hr. after the start of the run

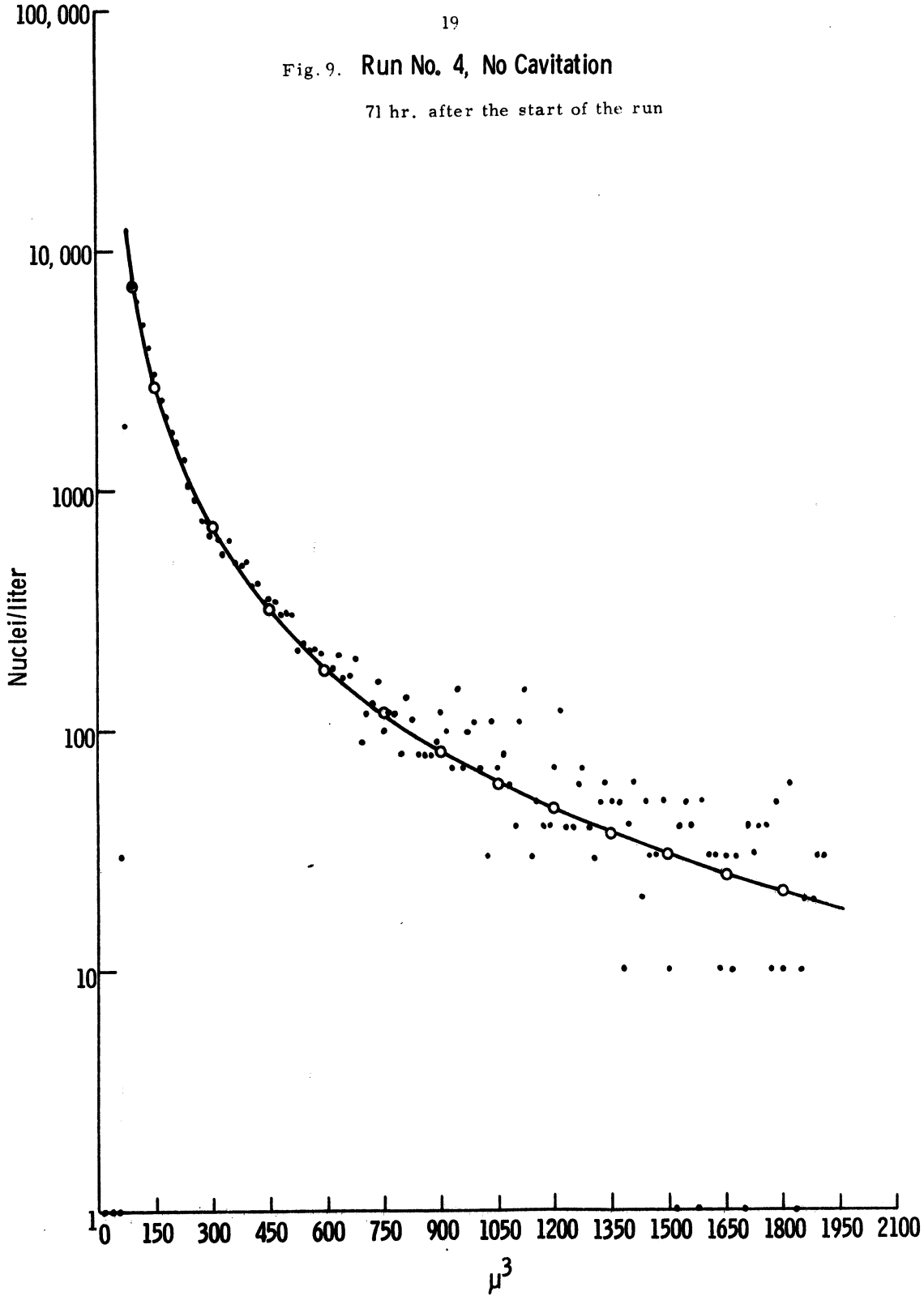

Fig. 10 **Run No. 5, No Cavitation**

96 hr. after the start of the run

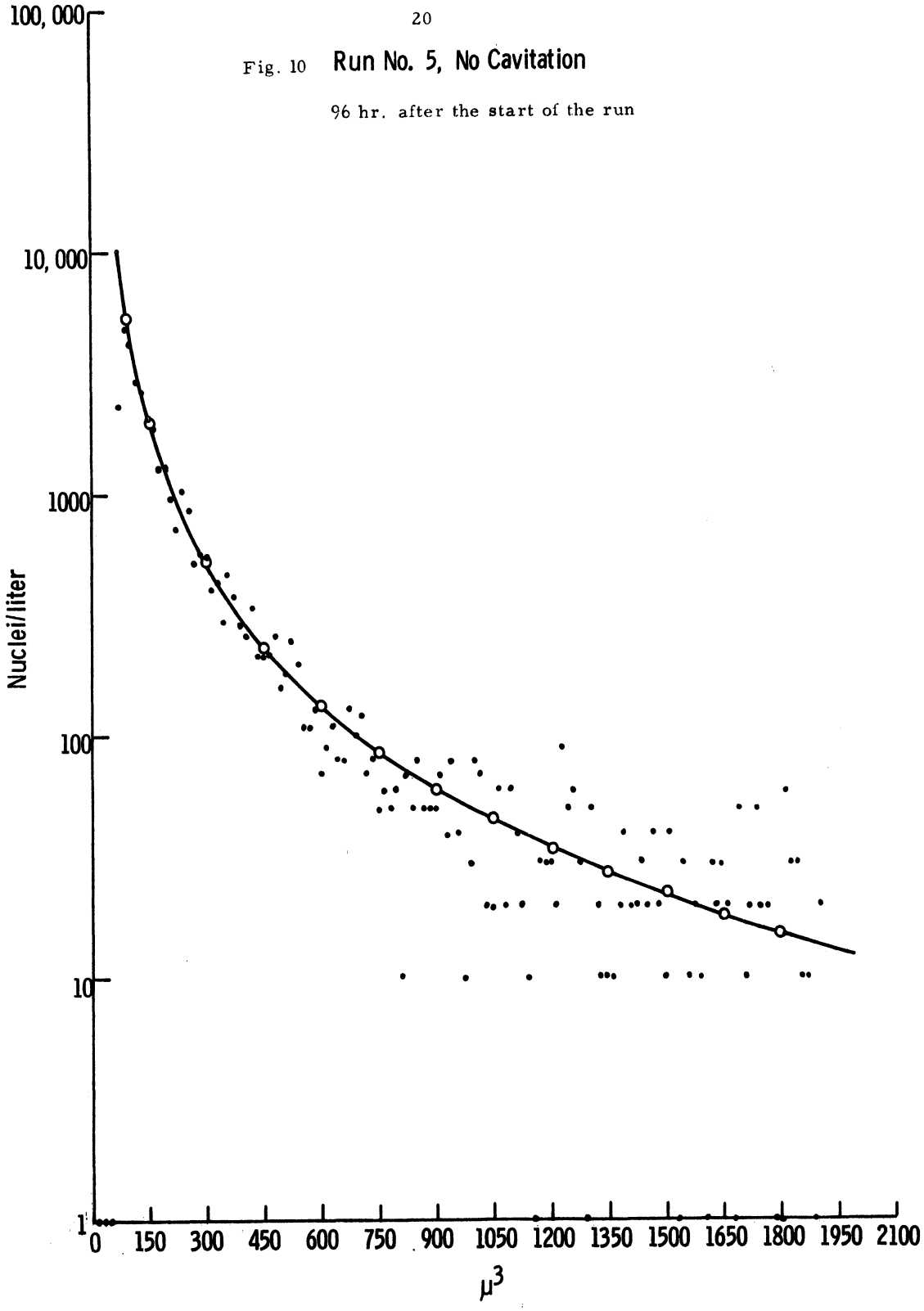

Fig. 11. **Run No. 6, No Cavitation**

118.67 hr. after the start of the run

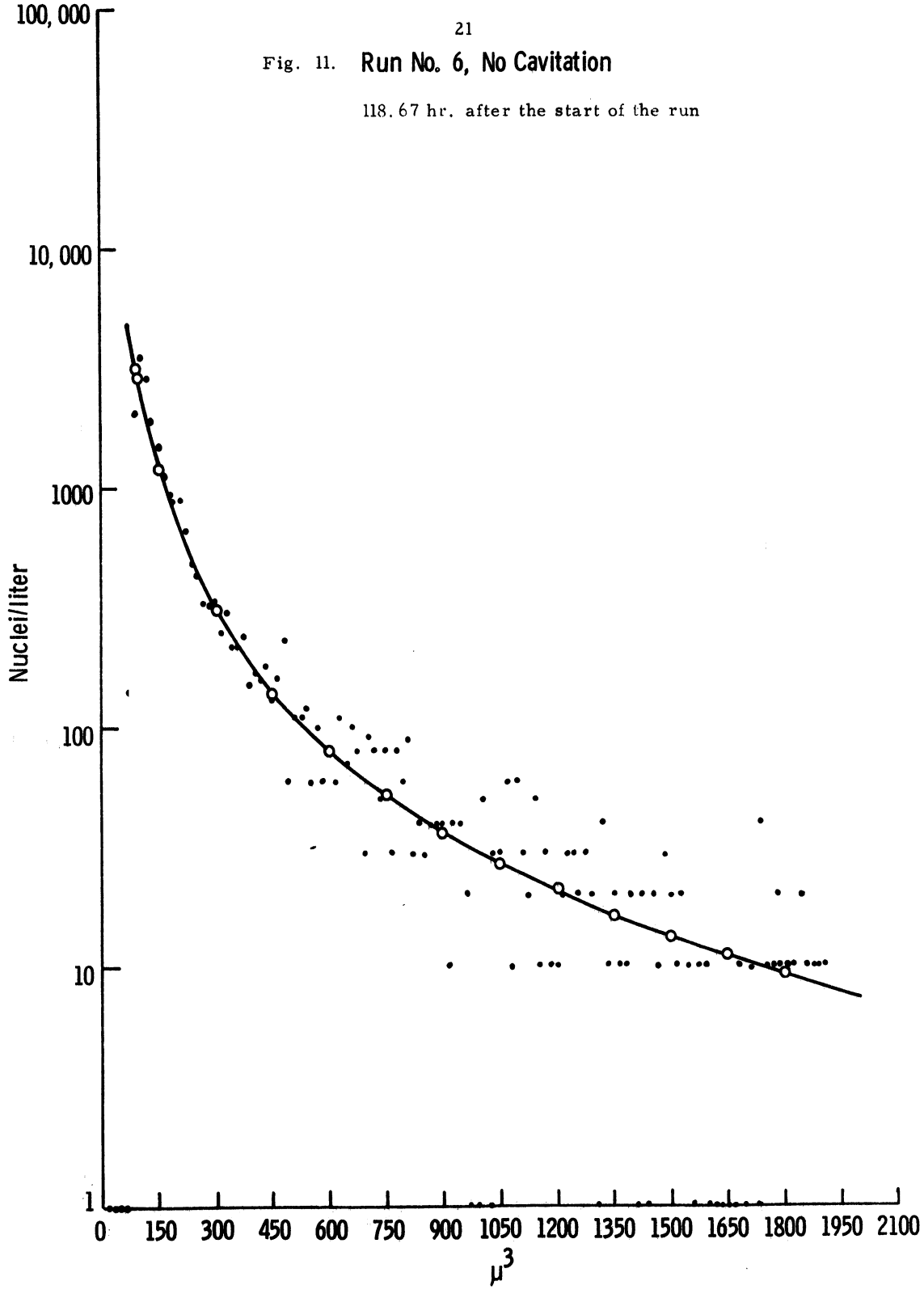

Fig. 12. **Run No. 7, No Cavitation**

142.50 hr. after the start of the run

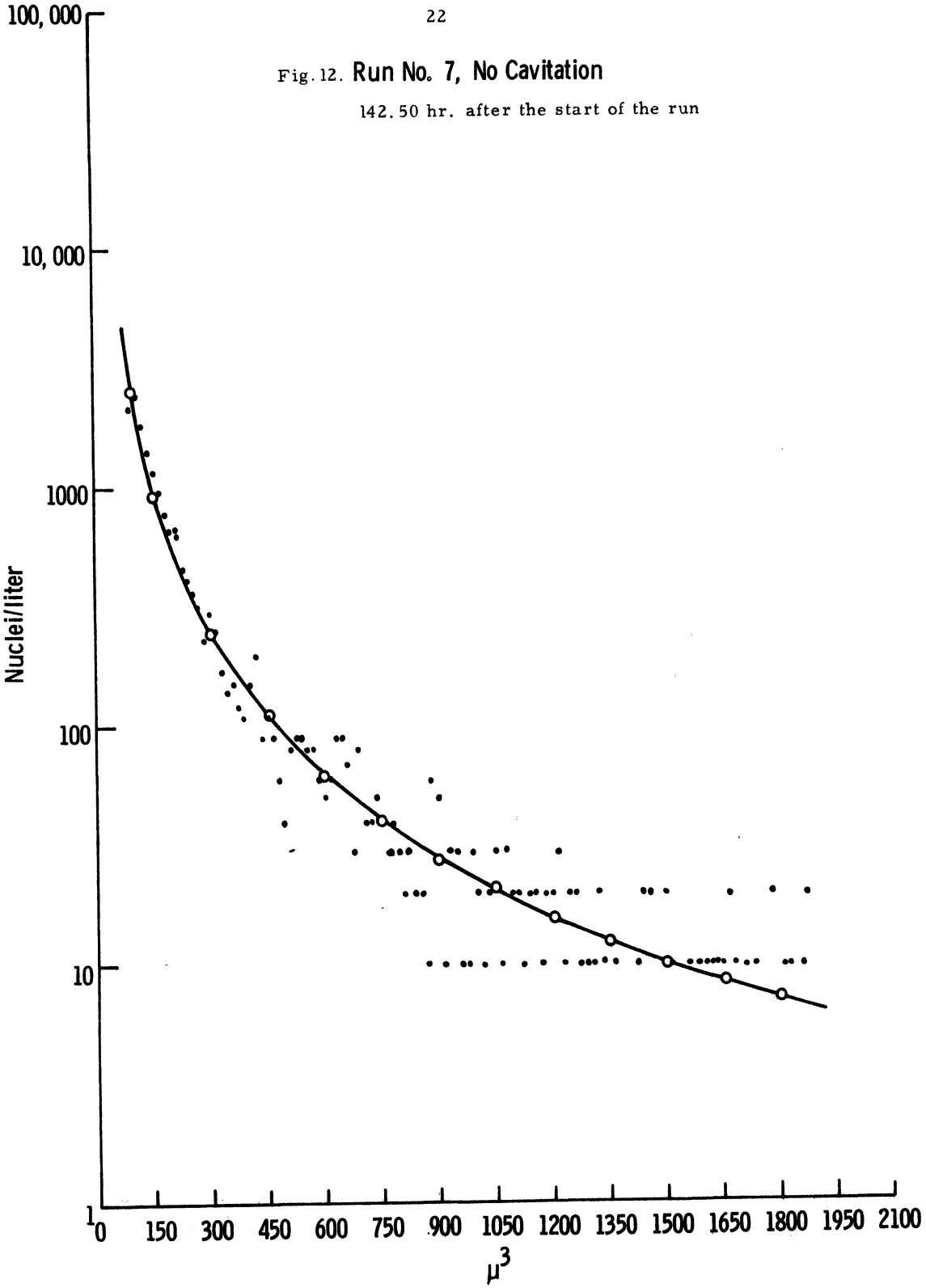

Fig. 13. **Run No. 8, No Cavitation**

166.8 hr. after the start of the run

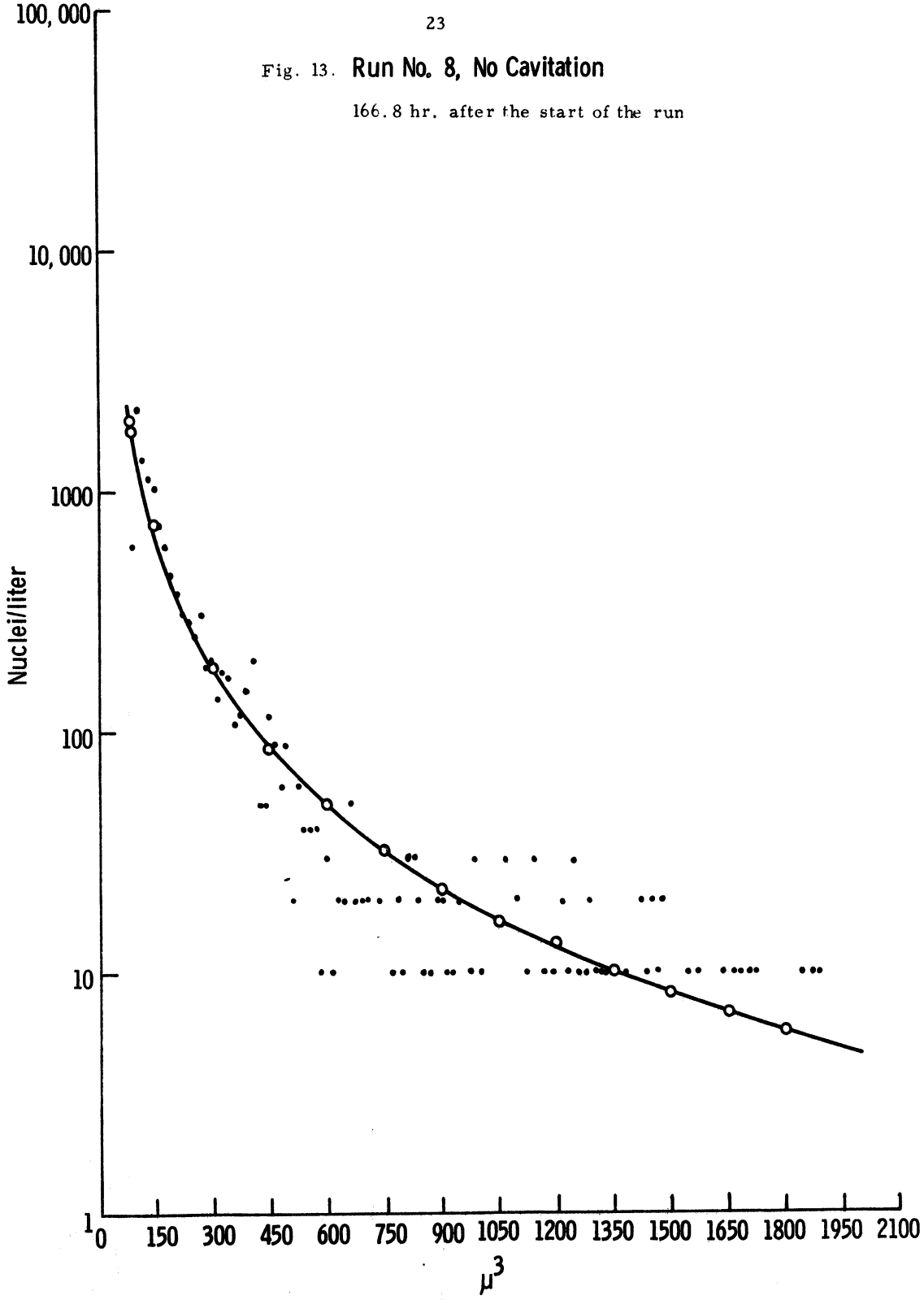

Fig. 14. **Run No. 9, No Cavitation**

190.67 hr. after the start of the run

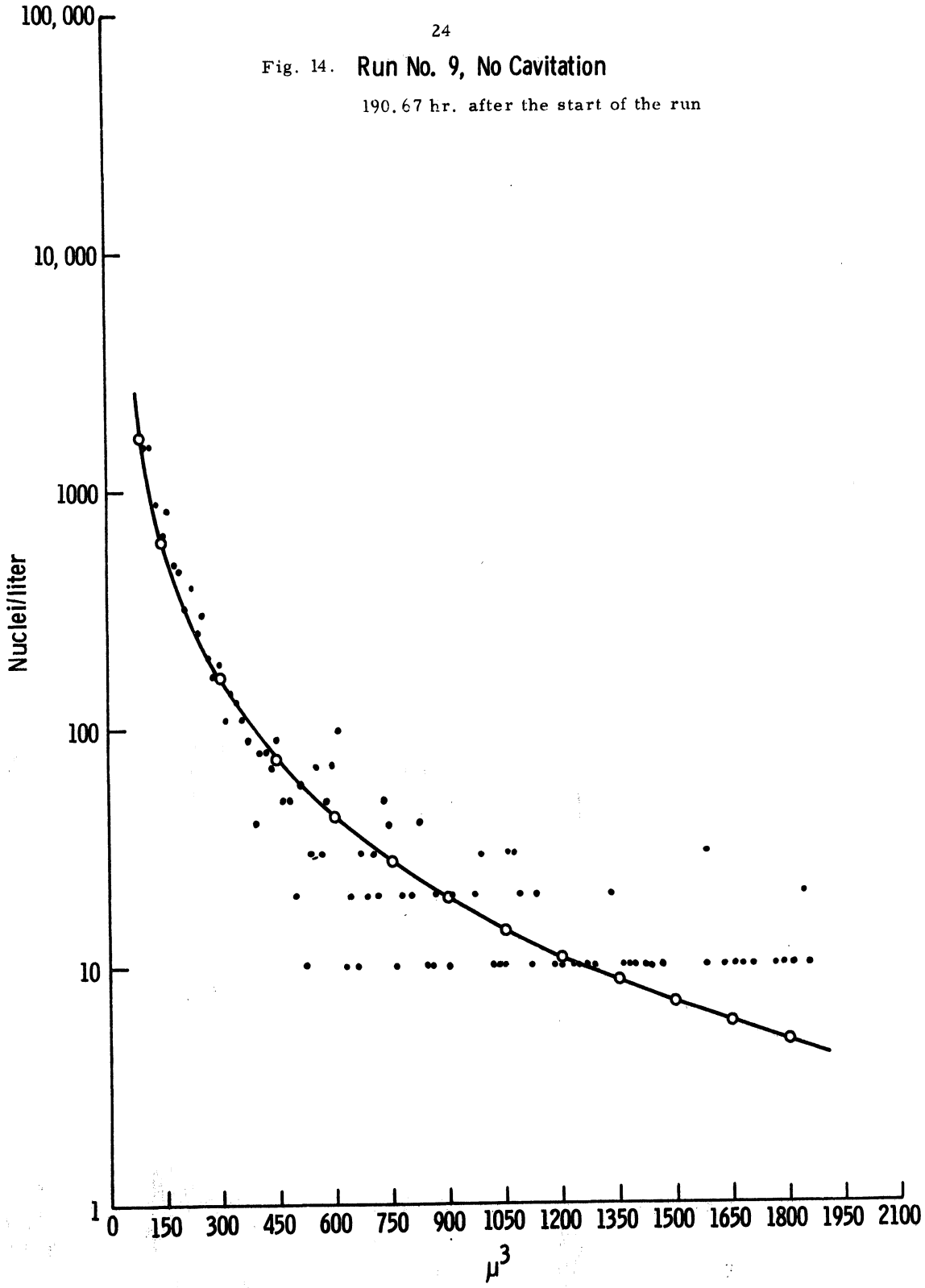

Fig. 15. **Run No. 10, No Cavitation**

213.42 hr. after the start of the run

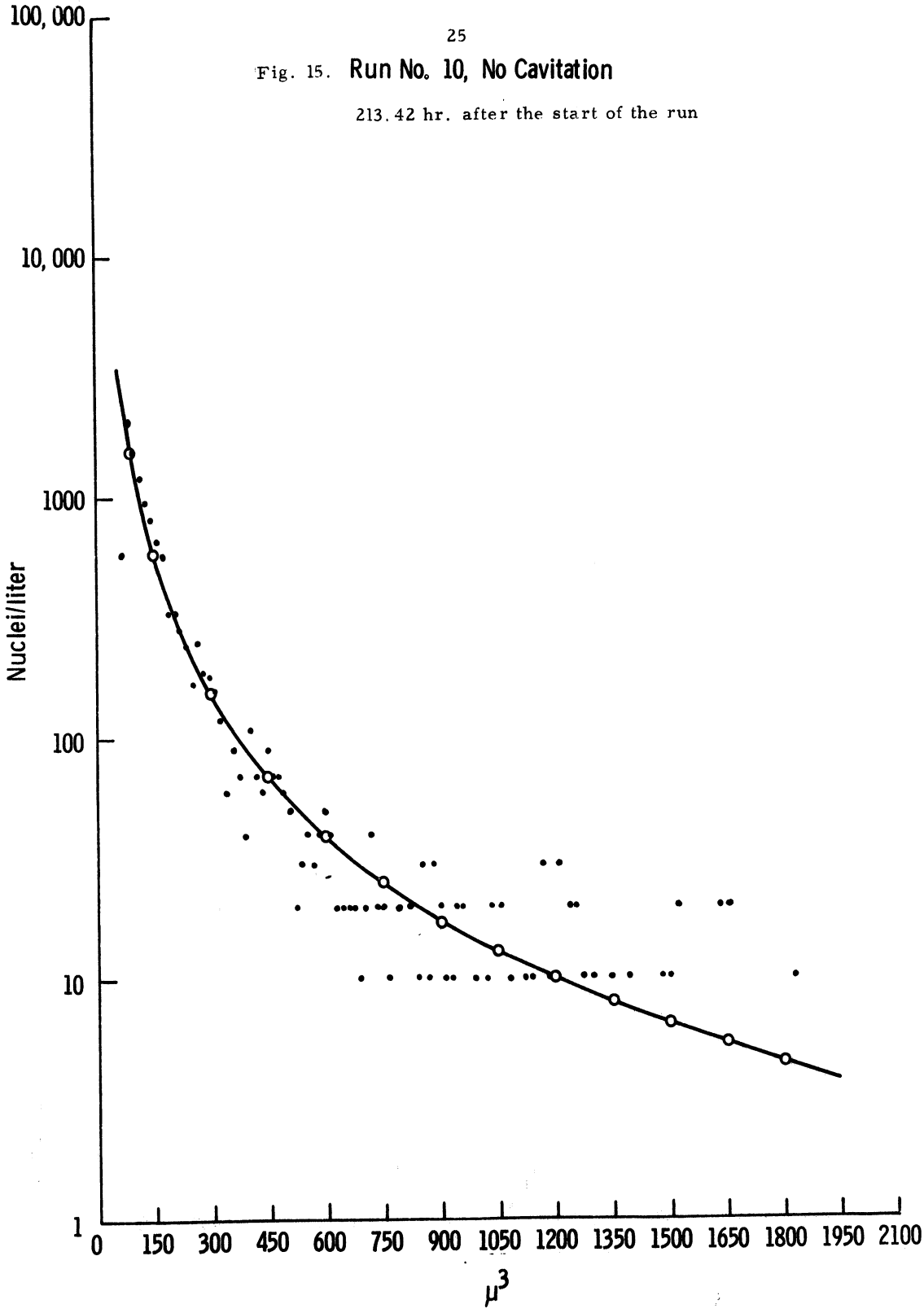

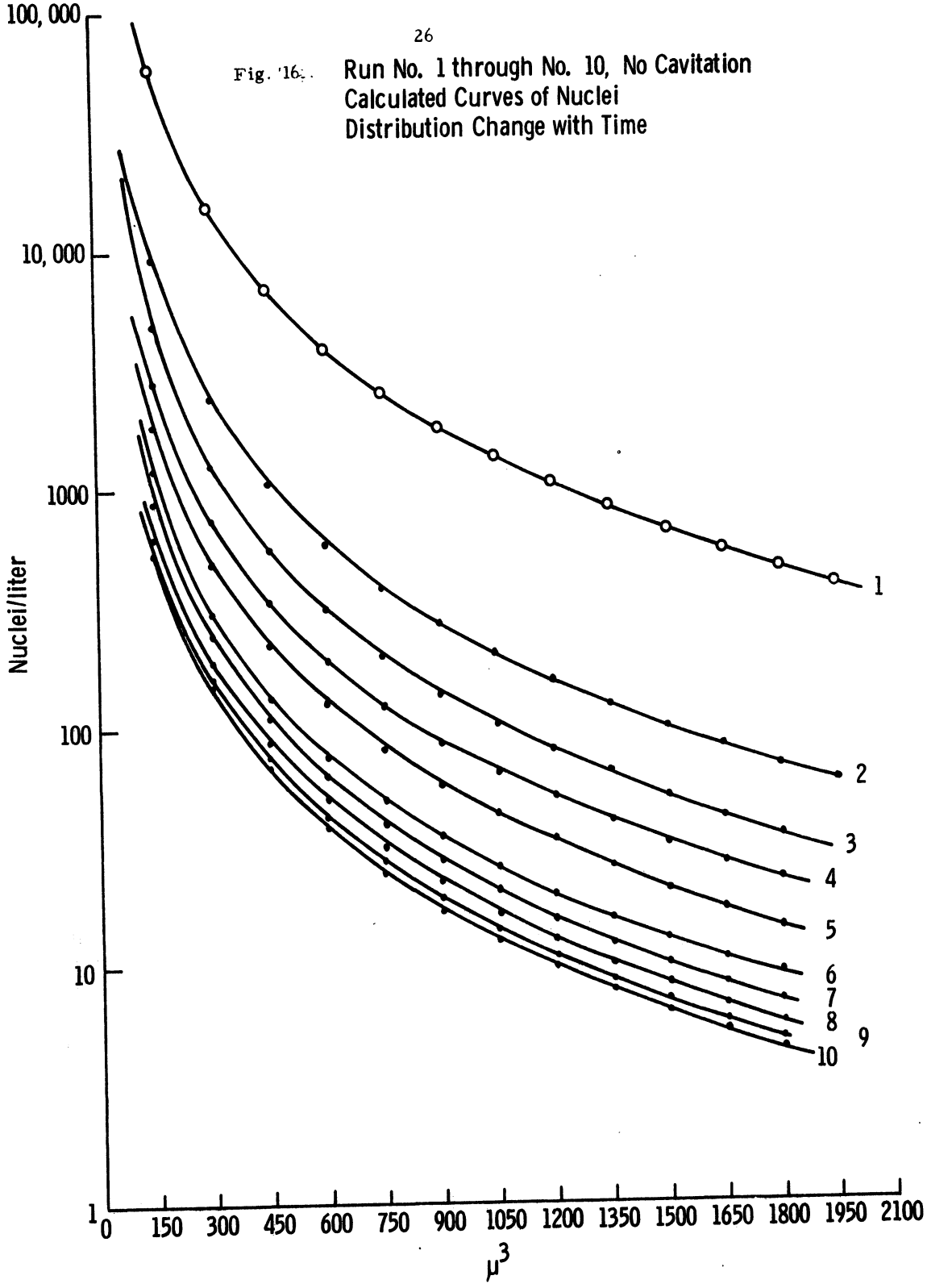

Fig. 16. Run No. 1 through No. 10, No Cavitation
Calculated Curves of Nuclei
Distribution Change with Time

Fig. 18. **Trial Run No. 2, No Cavitation Calculated Spectra**

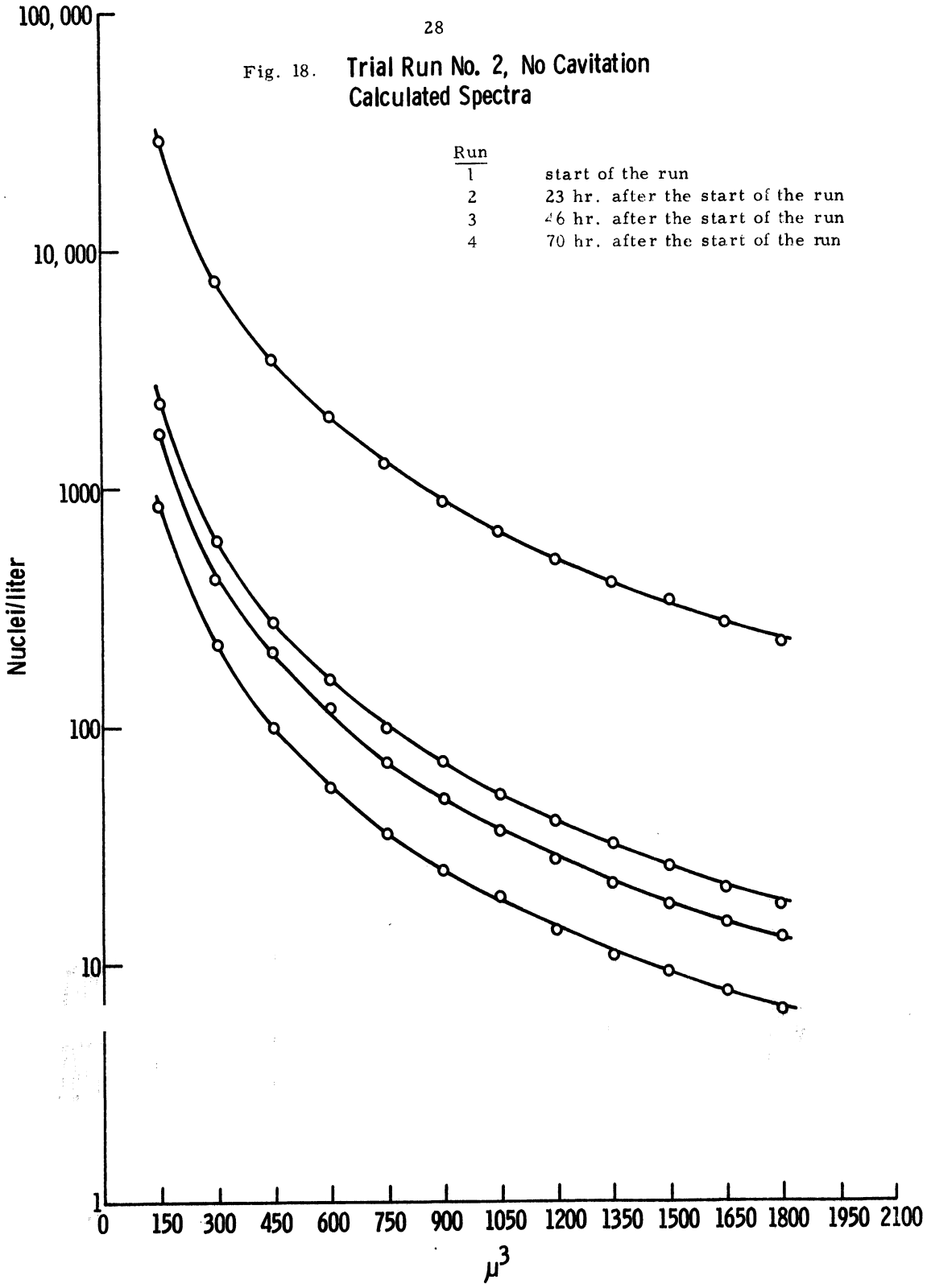

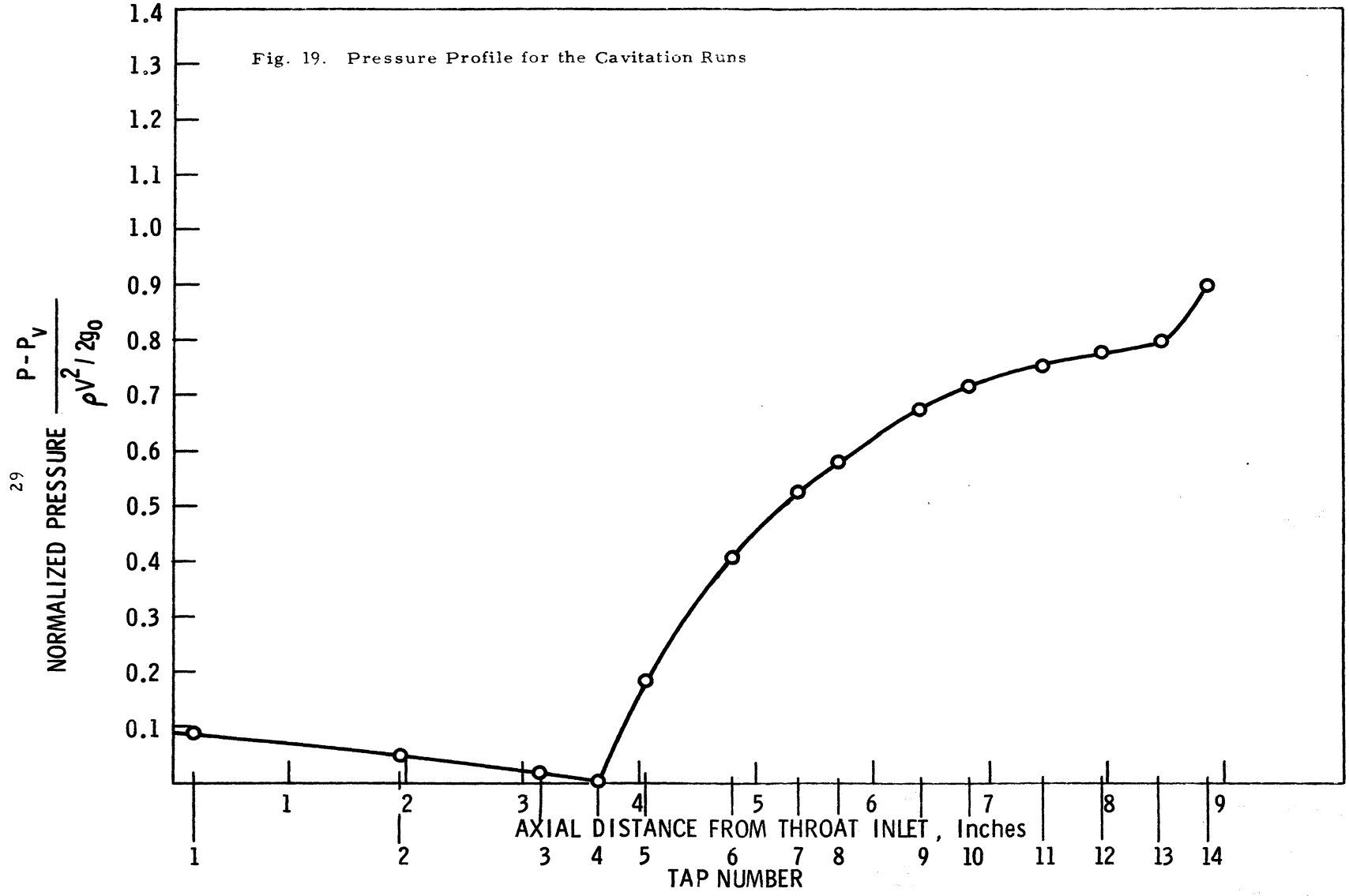

Fig. 19. Pressure Profile for the Cavitation Runs

Fig. 20. Cavitation, Run No. 1
2-Loops
Start of the run

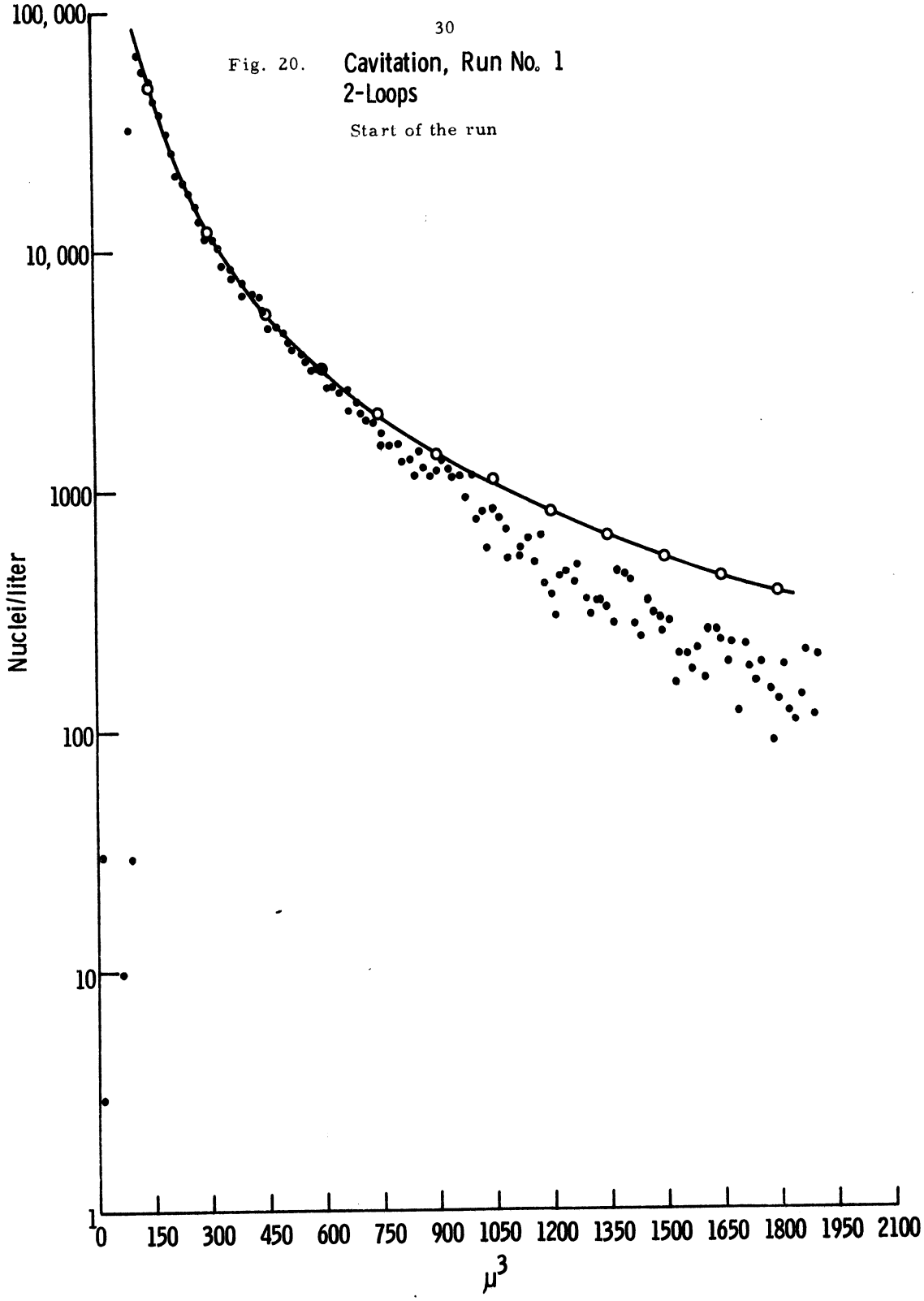

Fig. 21. **Cavitation, Run No. 2**
2-Loops
23.42 hr. after the start of the run

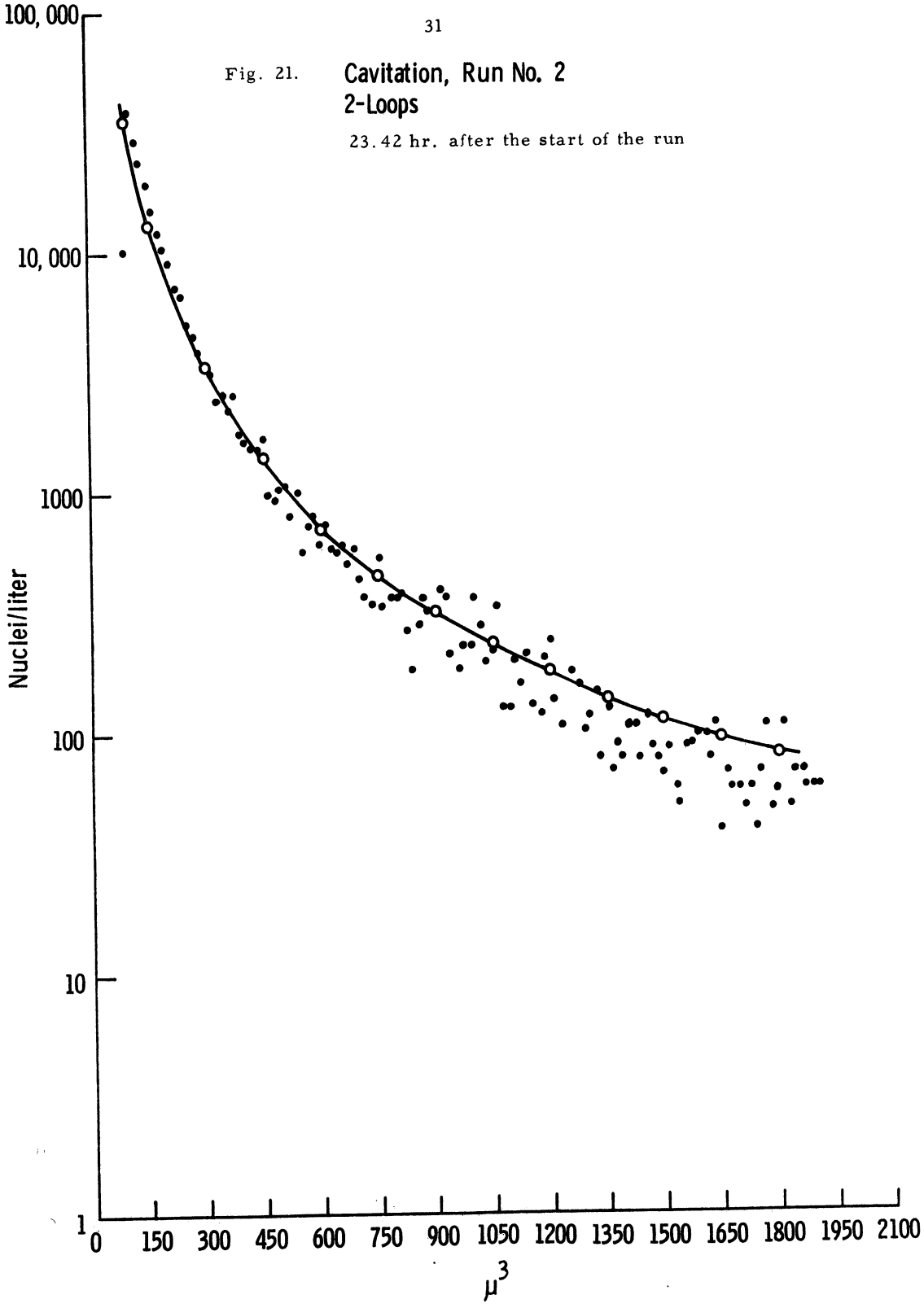

Fig. 22. **Cavitation, Run No. 3**
2-Loops

46.50 hr. after the start of the run

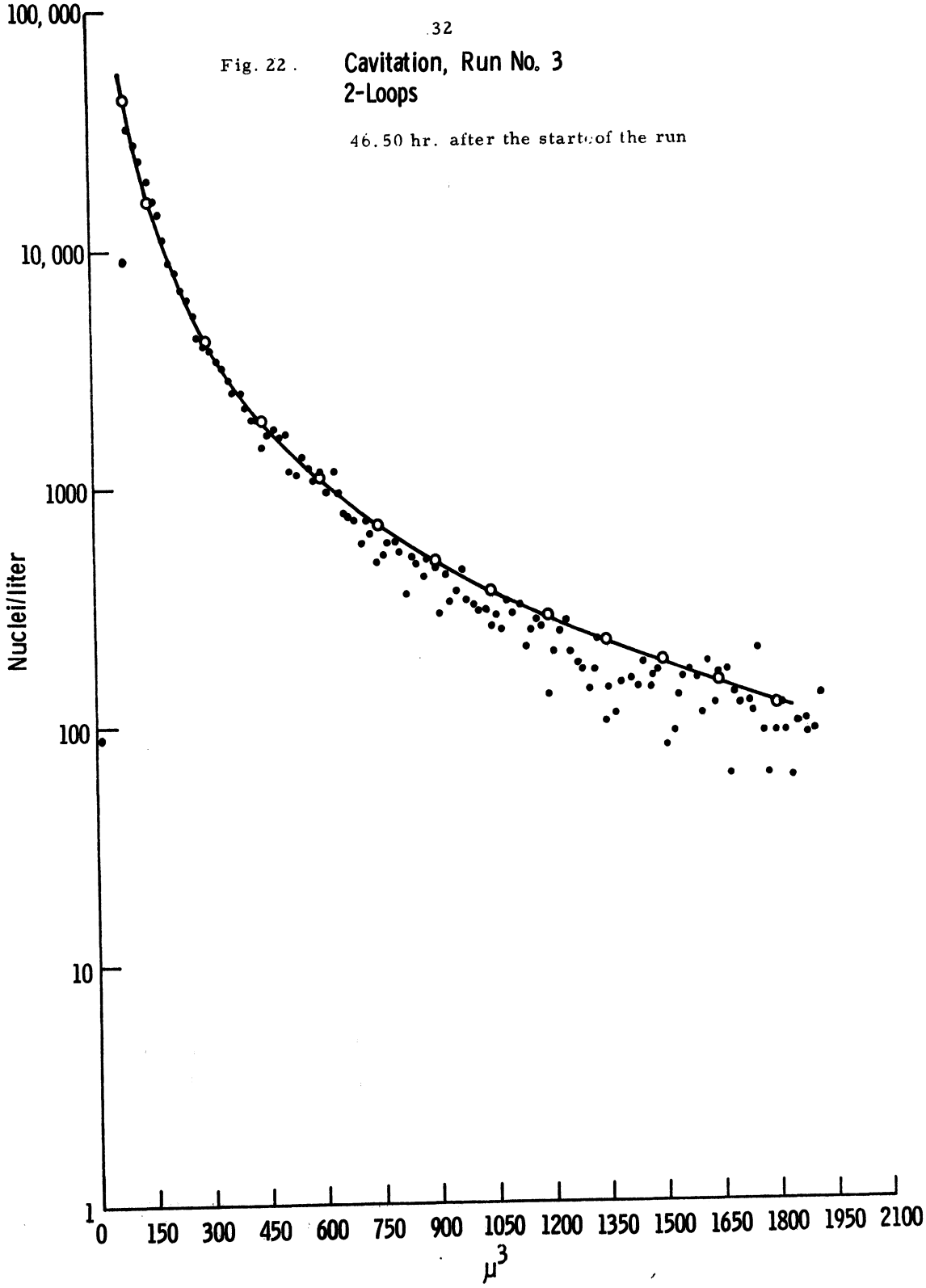

Fig. 23. **Cavitation, Run No. 4**
2-Loops

71.67 hr. after the start of the run

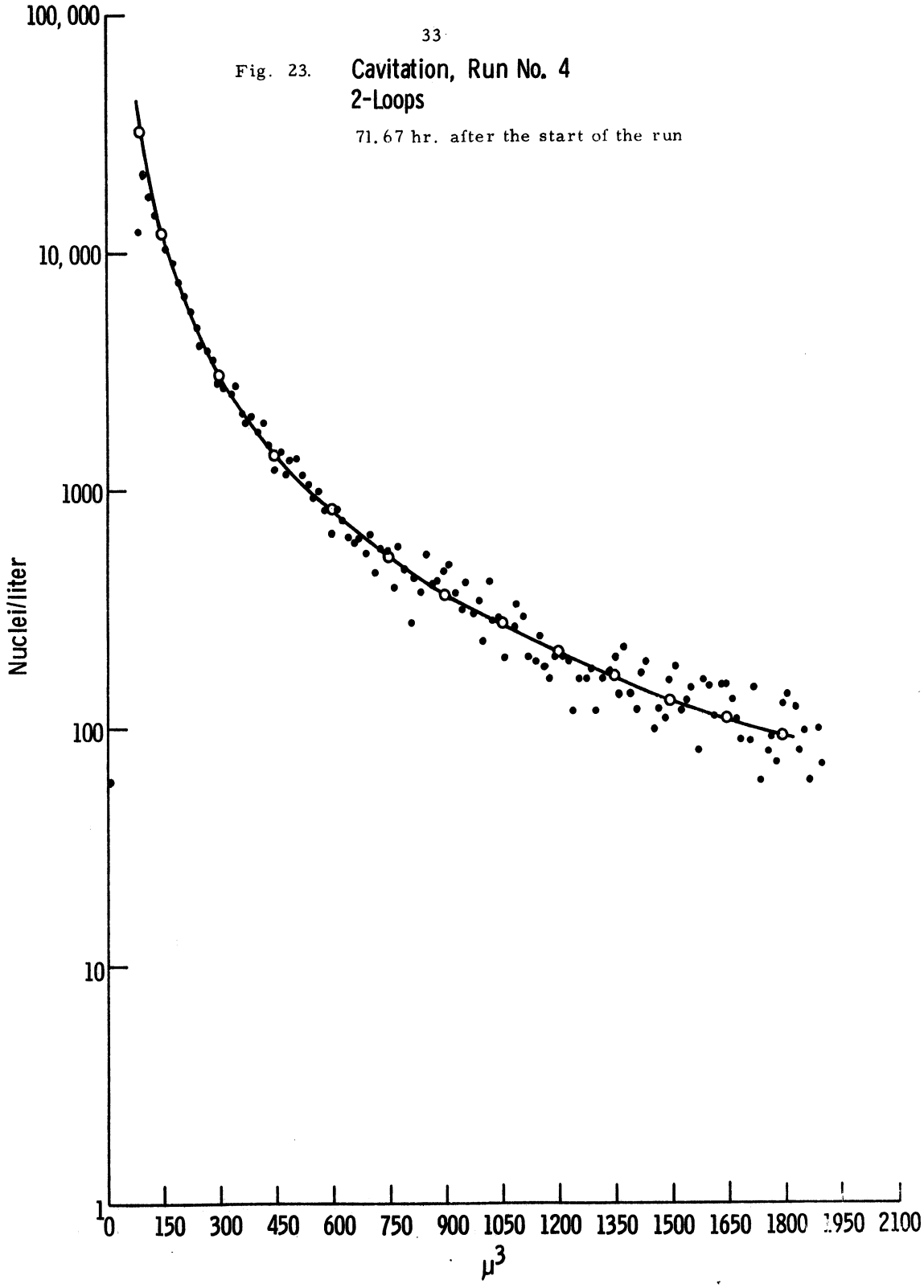

Fig. 24. **Cavitation, Run No. 5**
2-Loops

95.00 hr. after the start of the run

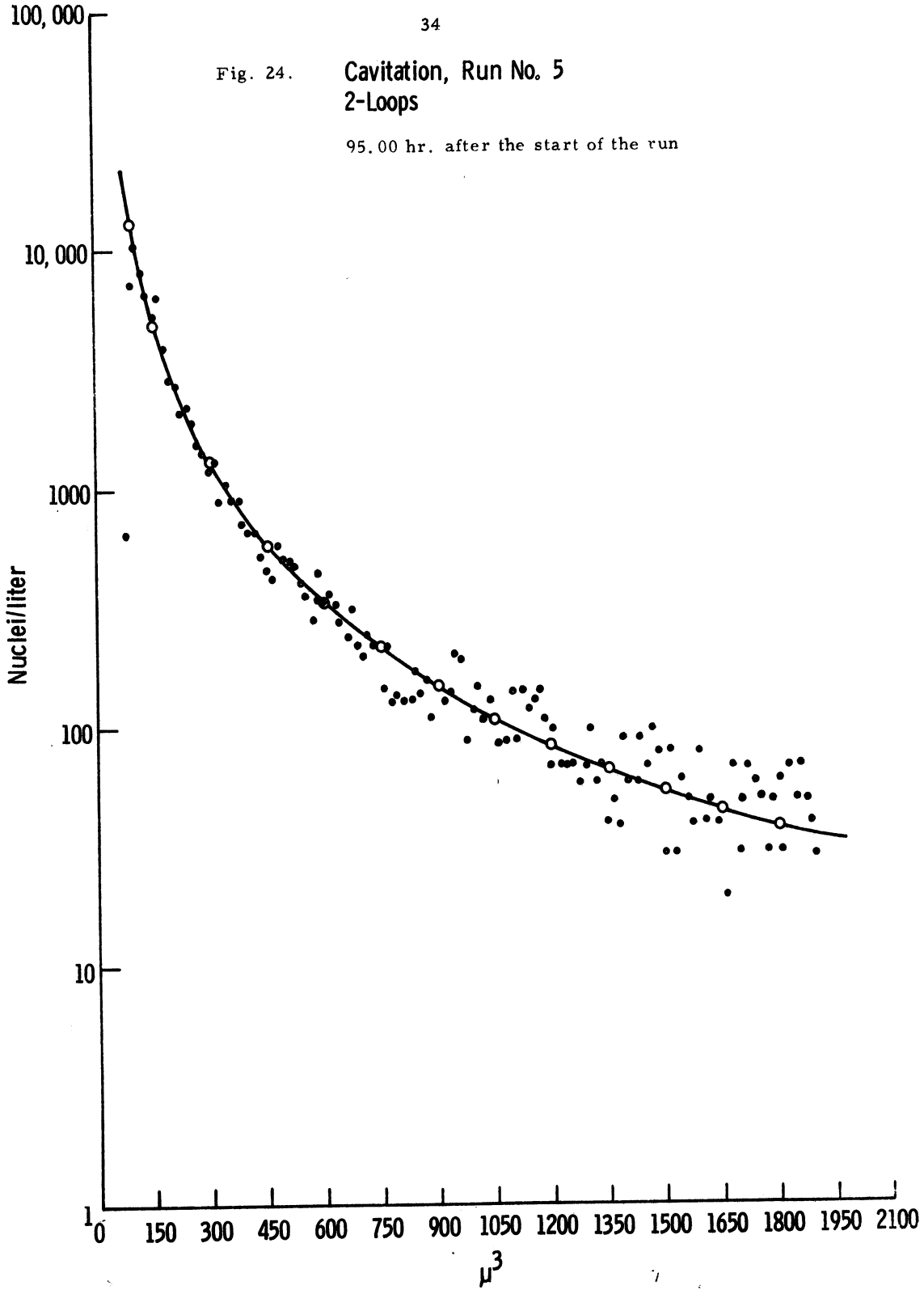

Fig. 25. **Cavitation, Run No. 6**
2-Loop

122.50 hr. after the start of the run

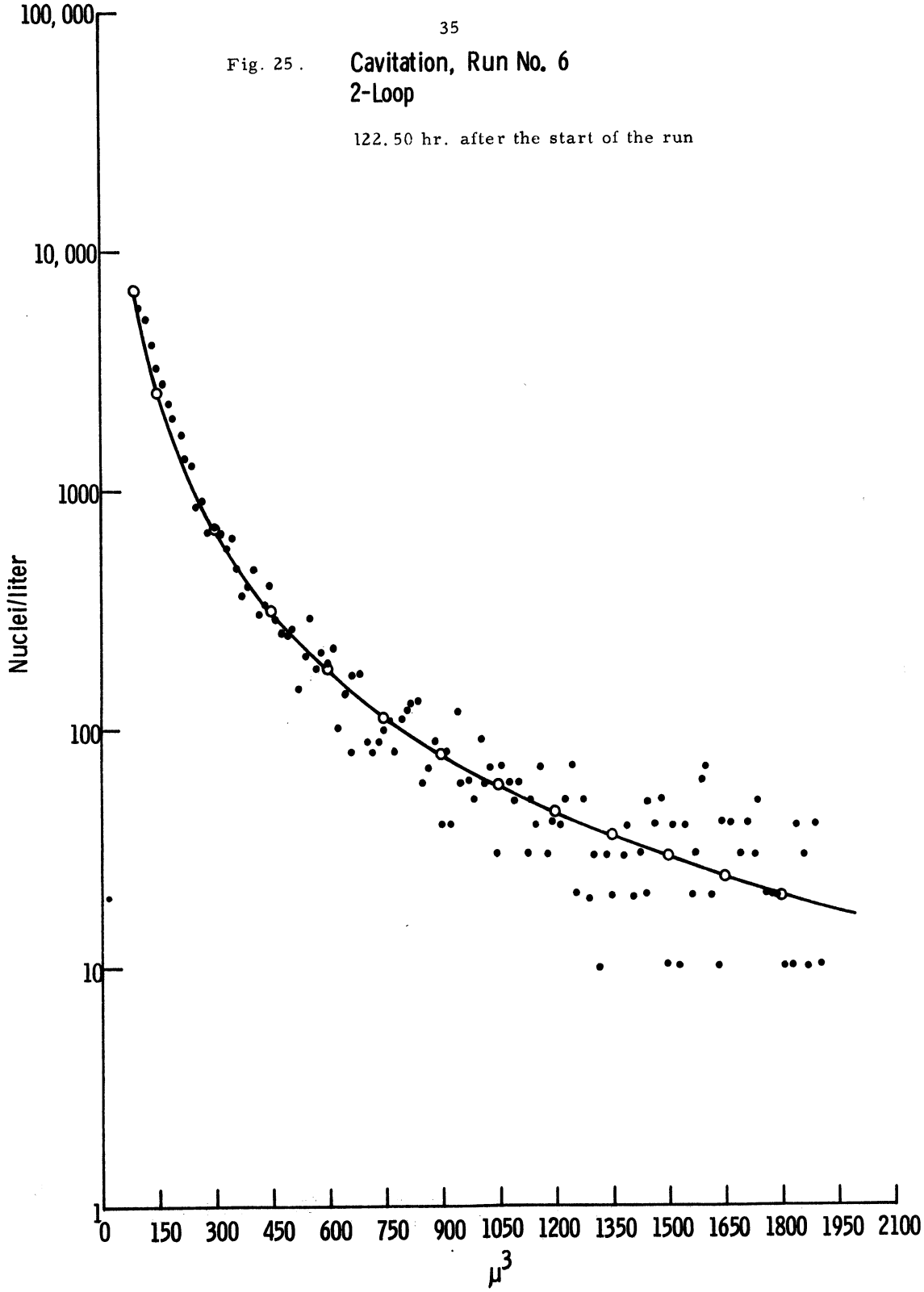

Fig. 26. Cavitation, Run No. 7
2-Loops
145.50 hr. after the start of the run

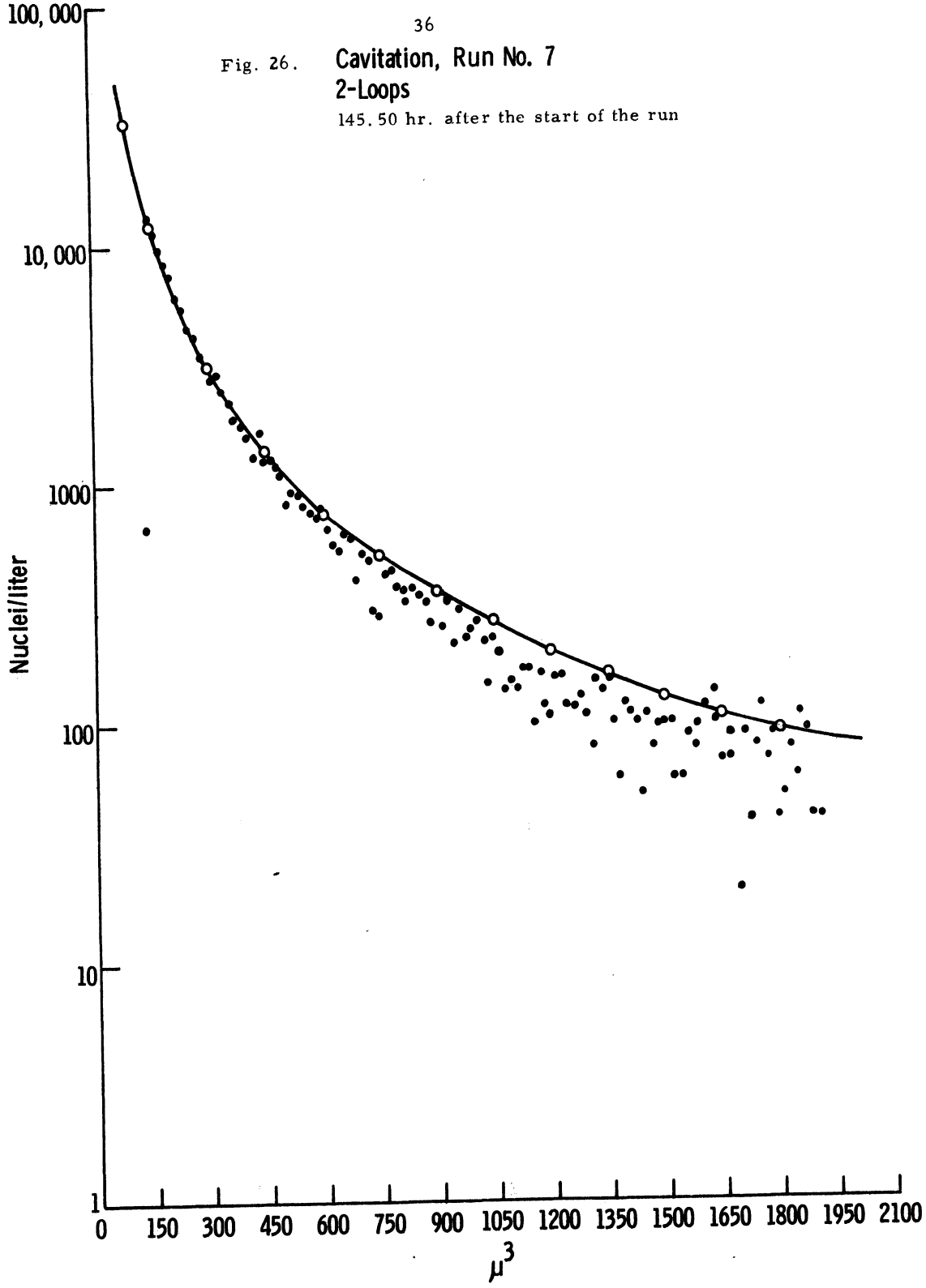

Fig. 27. **Cavitation, Run No. 8**
2-Loops

165.50 hr. after the start of the run

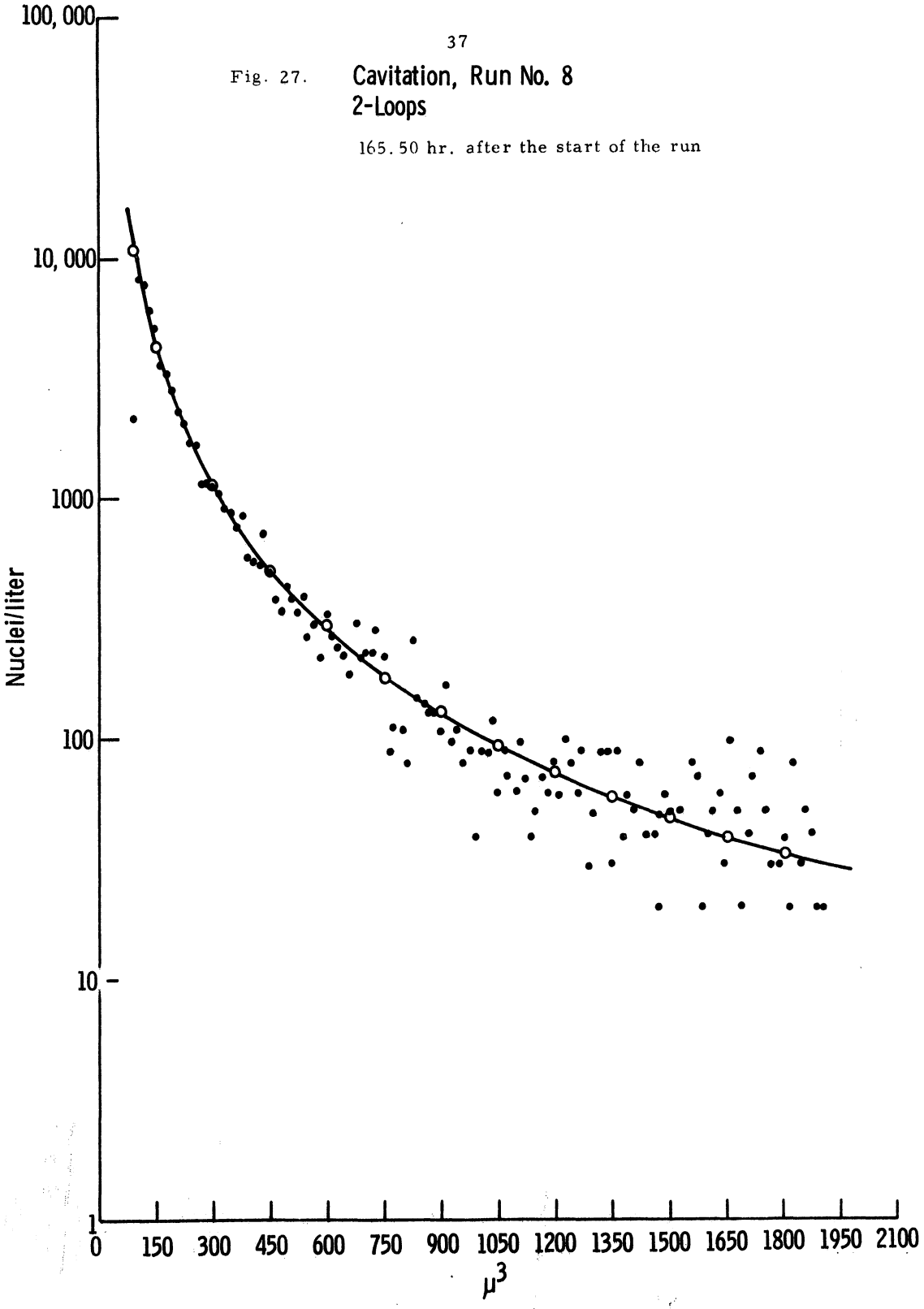

Fig. 28. Cavitation, Run No. 9
2-Loops

186.50 hr. after the start of the run

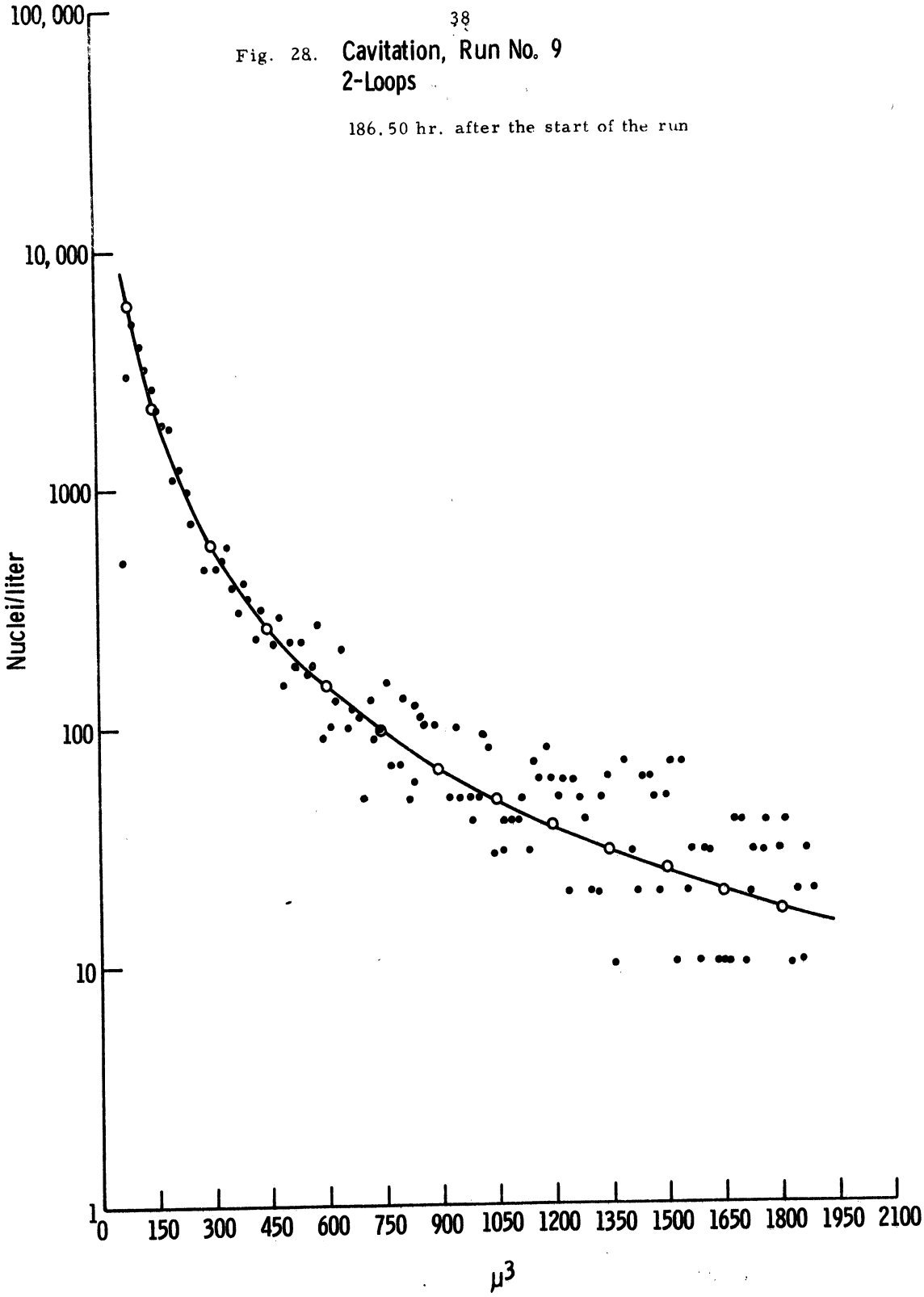

Fig. 29. **Cavitation, Run No. 10**

214.50 hr. after the start of the run

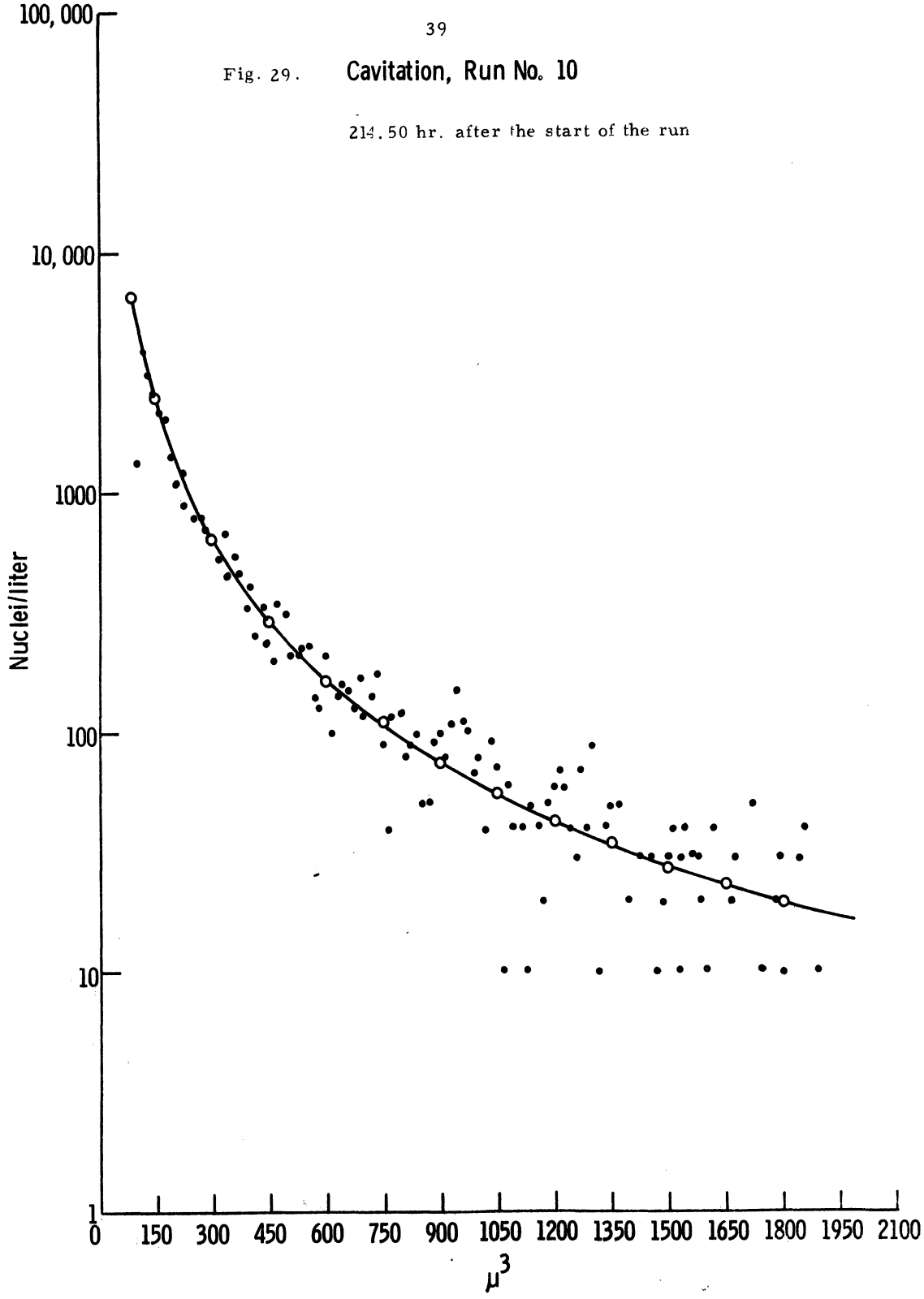

Fig. 30. Cavitation, Run No. 11

238.67 hr. after the start of the run

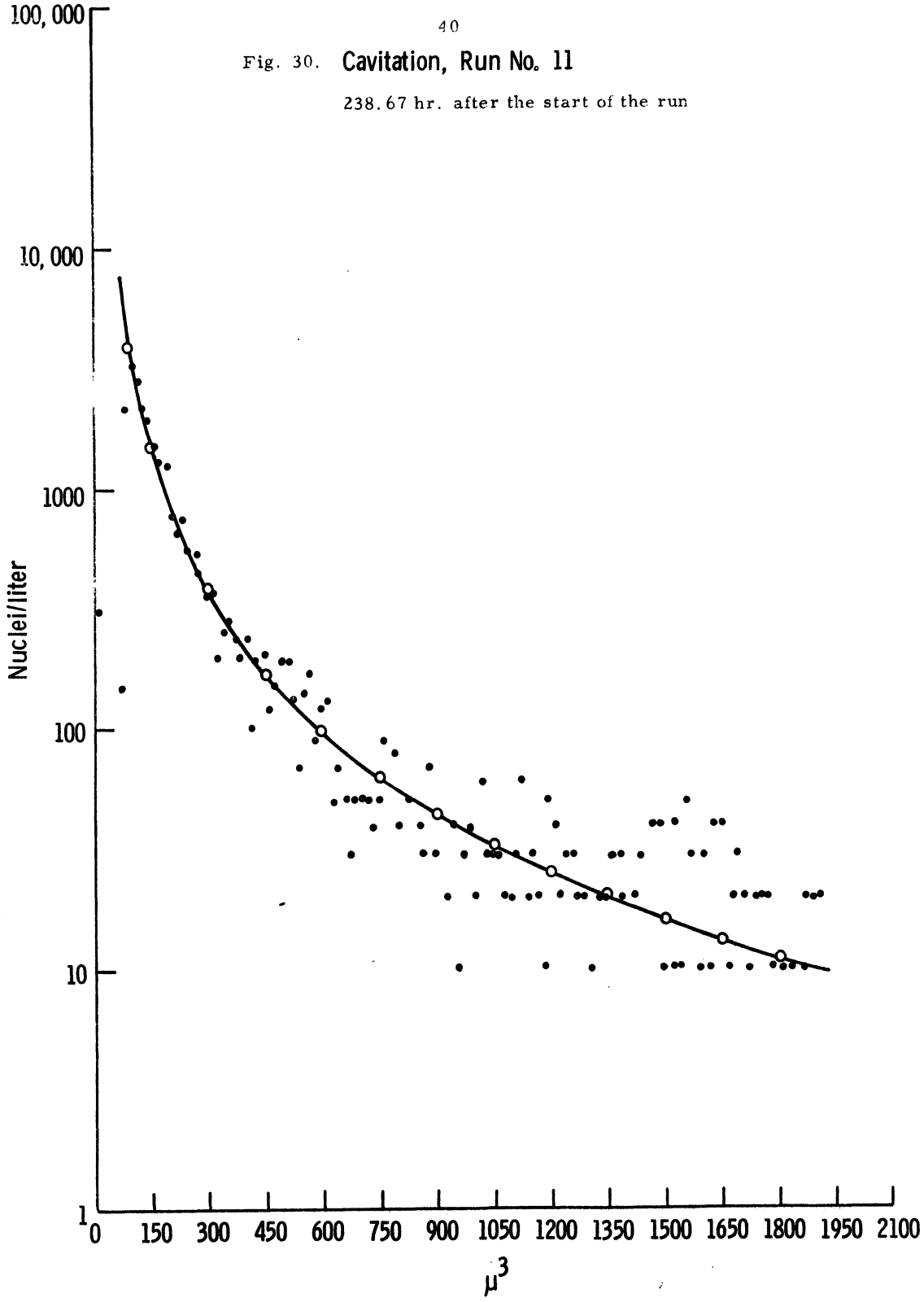

Fig. 31. Cavitation, Runs No. 1 through No. 11
2-Loops

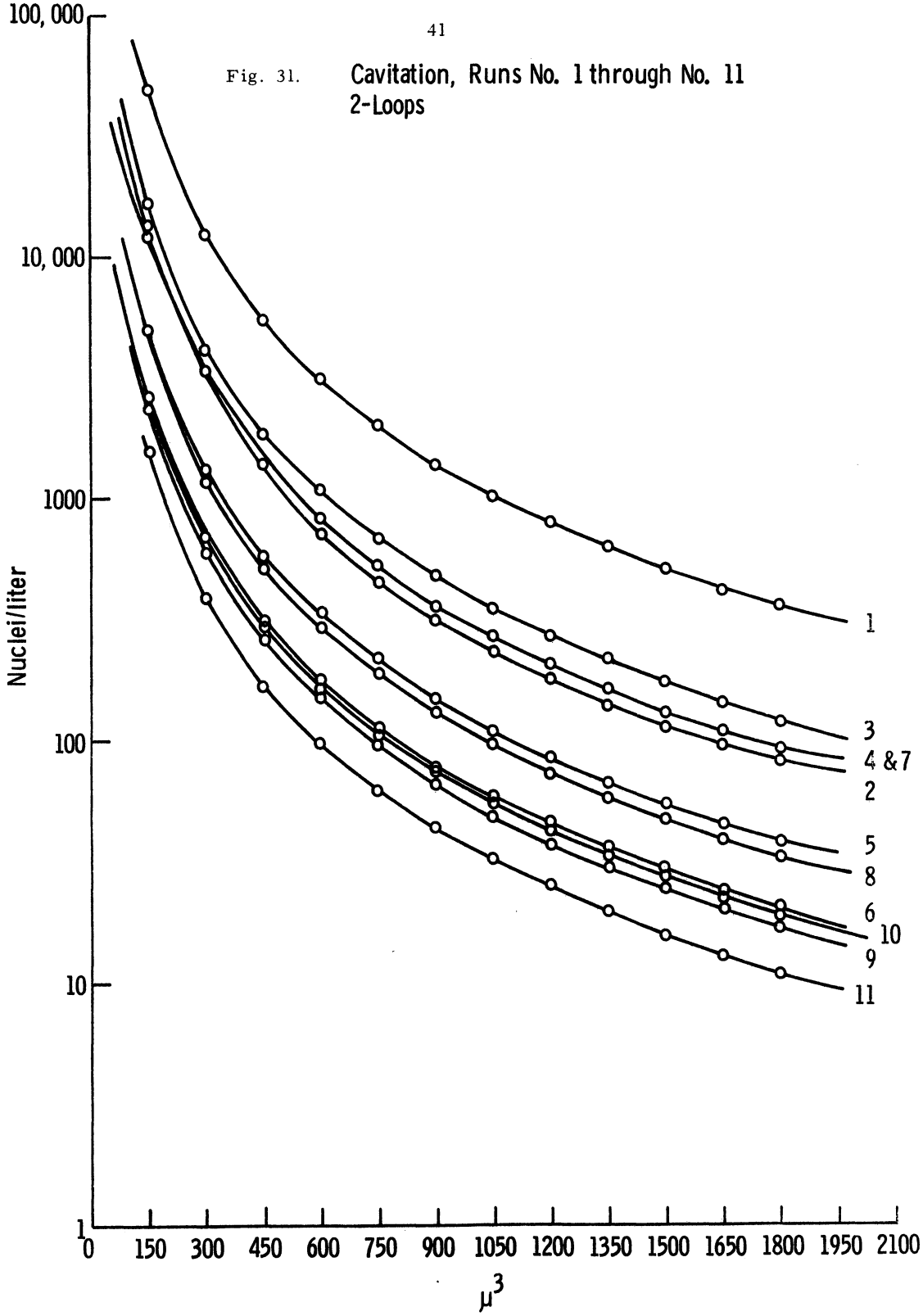

Fig. 32.. Run No. 1, Cavitation, 1-Loop

Start of the run

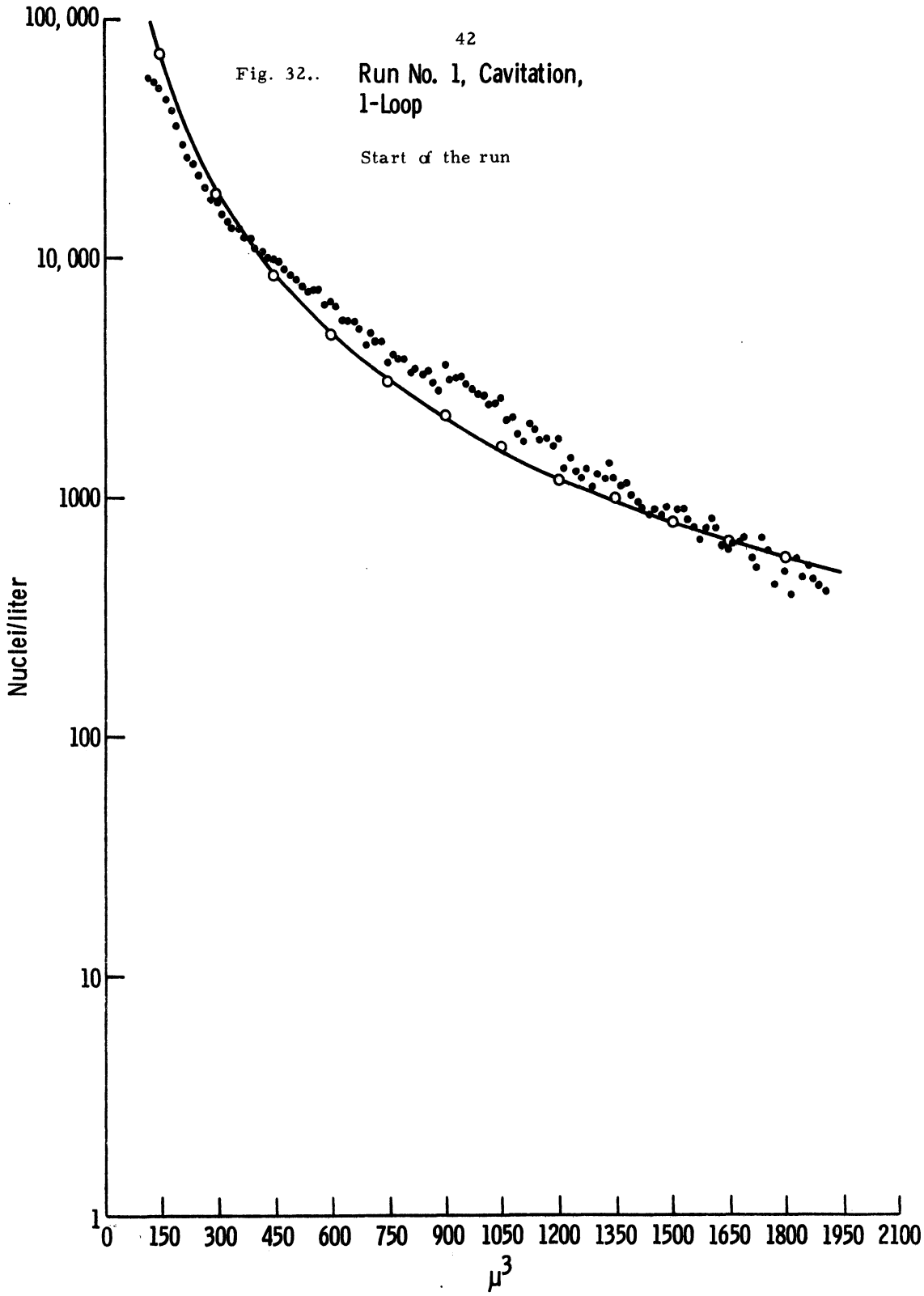

Fig. 33. Run No. 2, Cavitation, 1-Loop

24 hr. after the start of the run

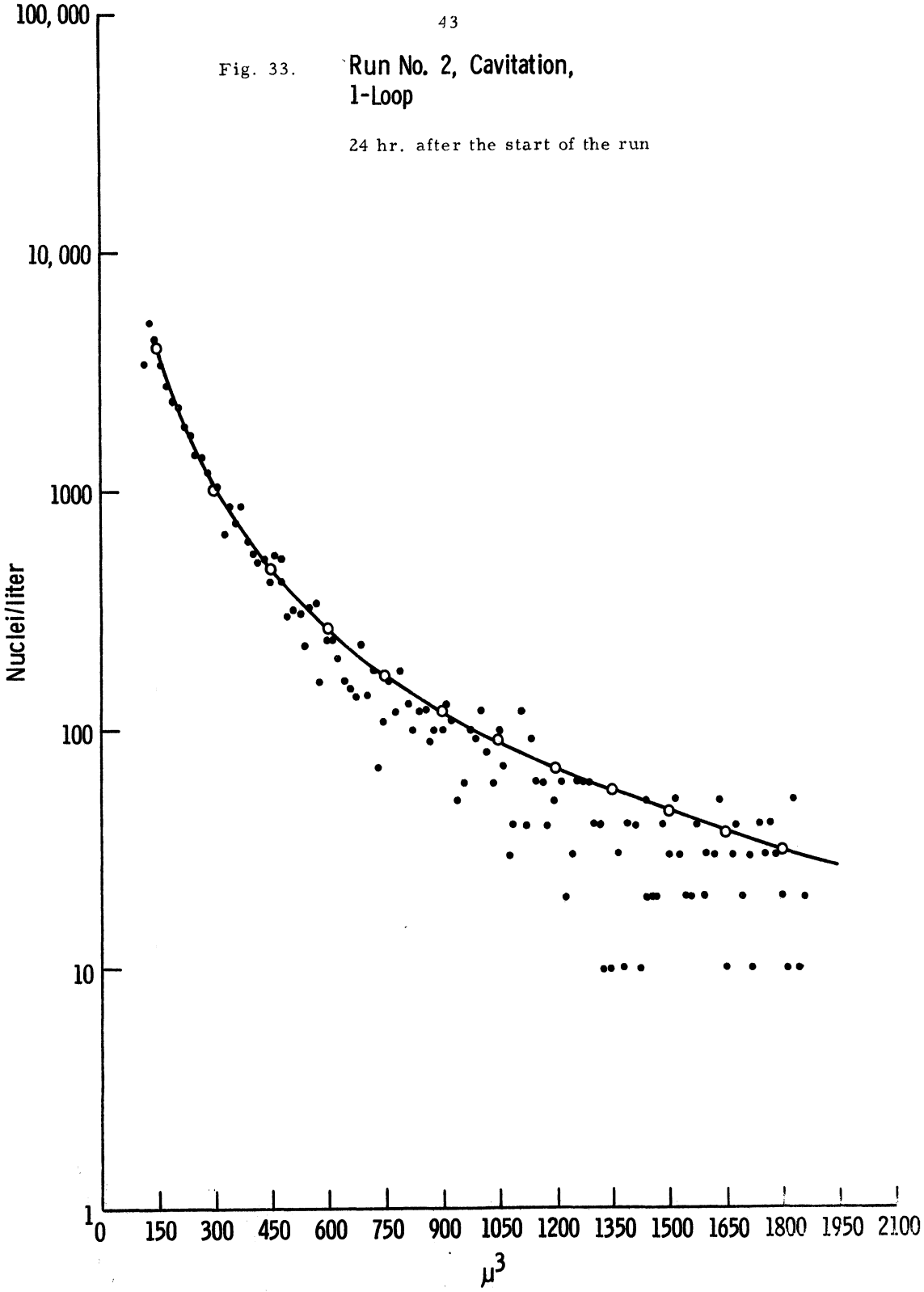

Fig. 34. Run No. 3, Cavitation, 1-Loop

48 hr. after the start of the run

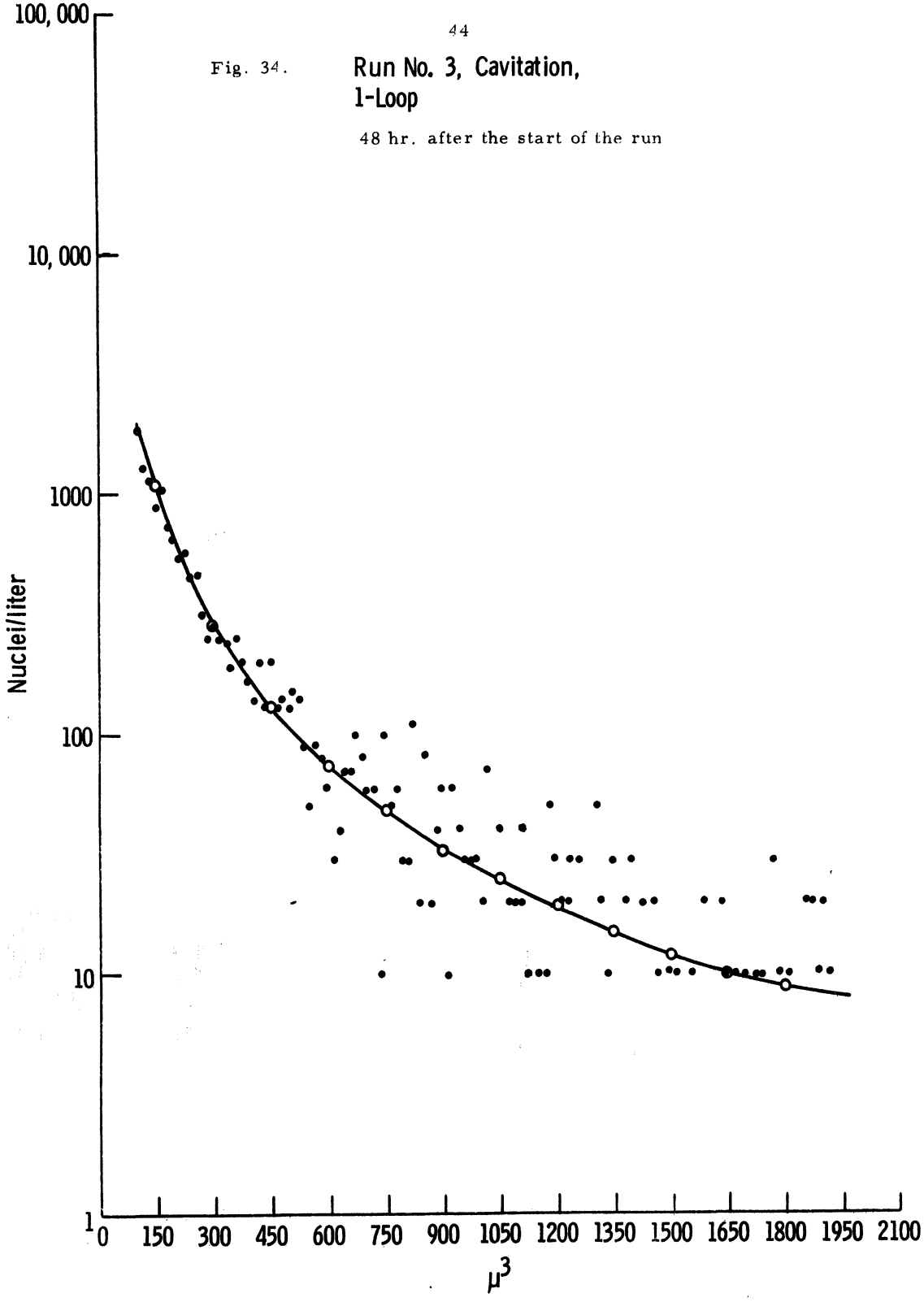

Fig. 35. **Run No. 4, Cavitation, 1-Loop**

71.50 hr. after the start of the run

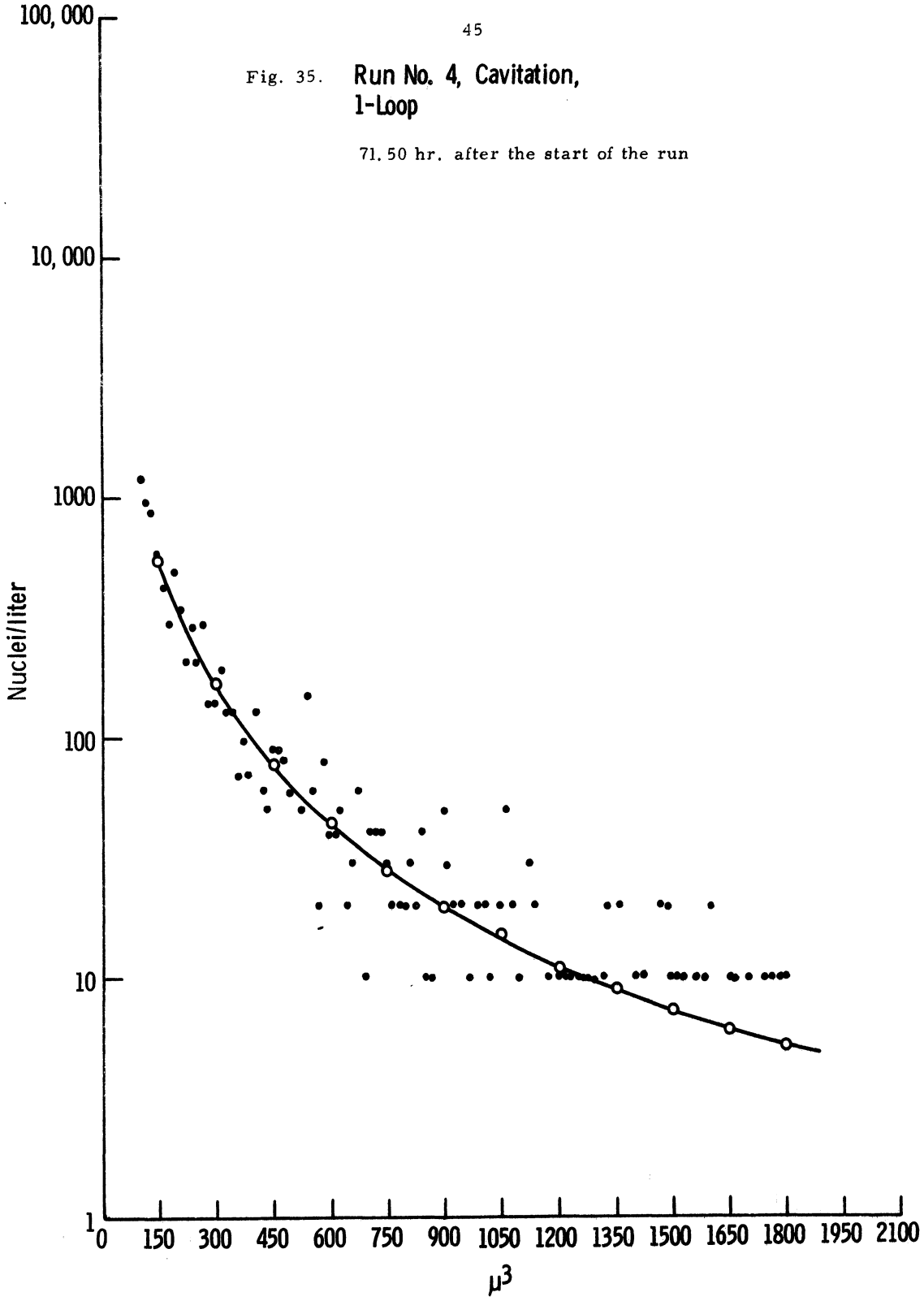

Fig. 36. **Run No. 5, Cavitation, 1-Loop**

96 hr. after the start of the run

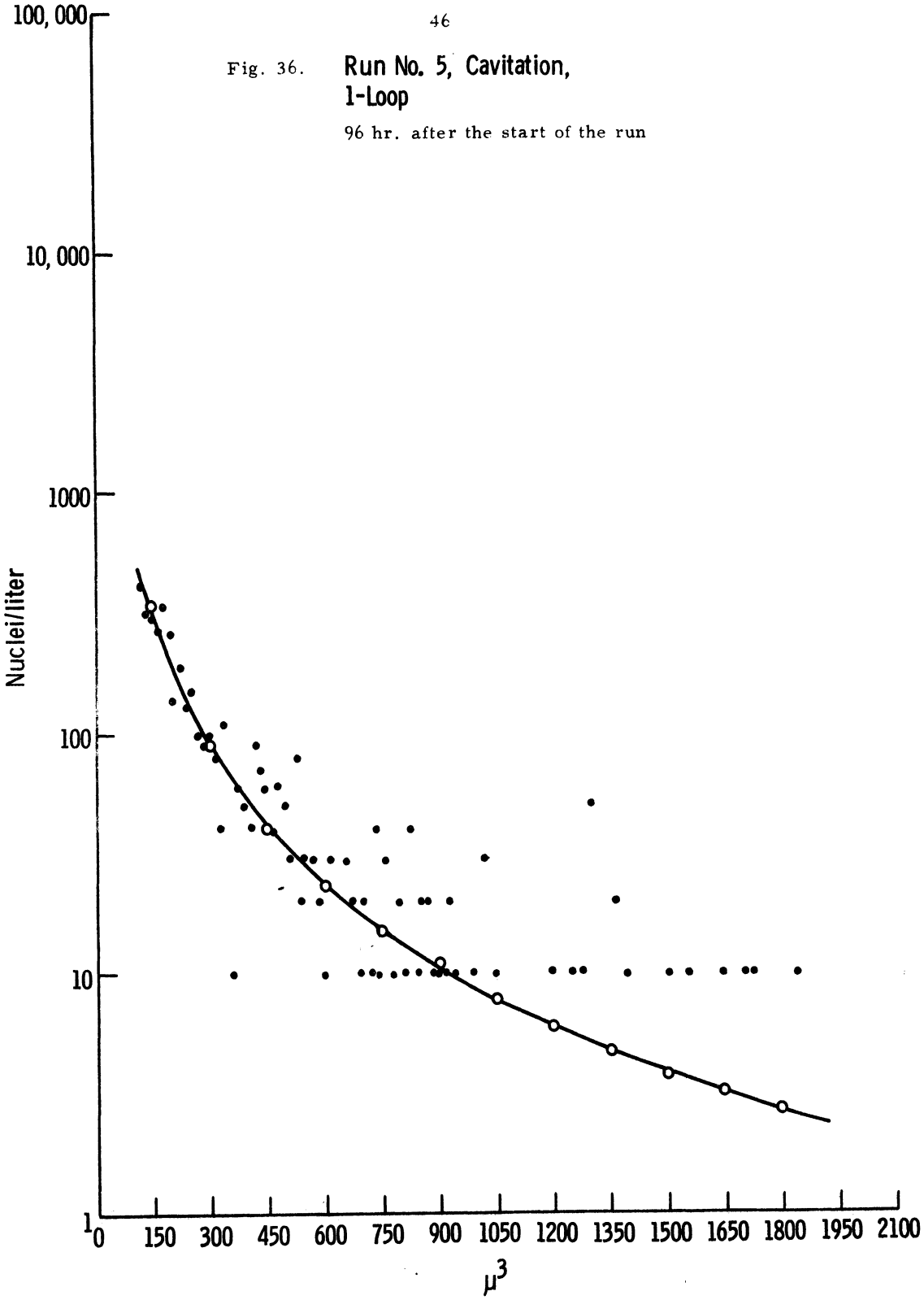

Fig. 37. **Run No. 6, Cavitation, 1-Loop**

119.50 hr. after the start of the run

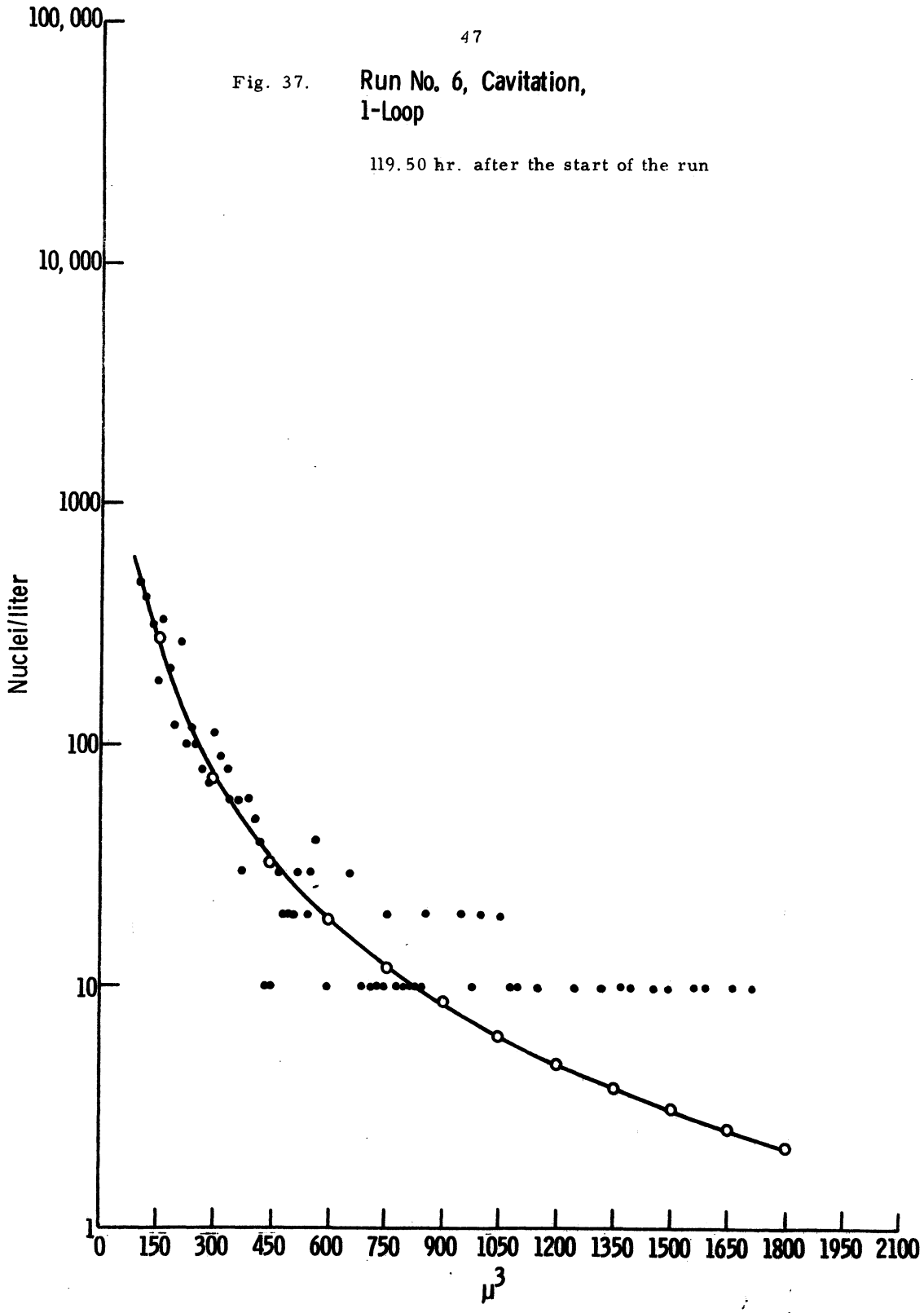

Fig. 38. **Run No. 7, Cavitation, 1-Loop**

144.50 hr. after the start of the run

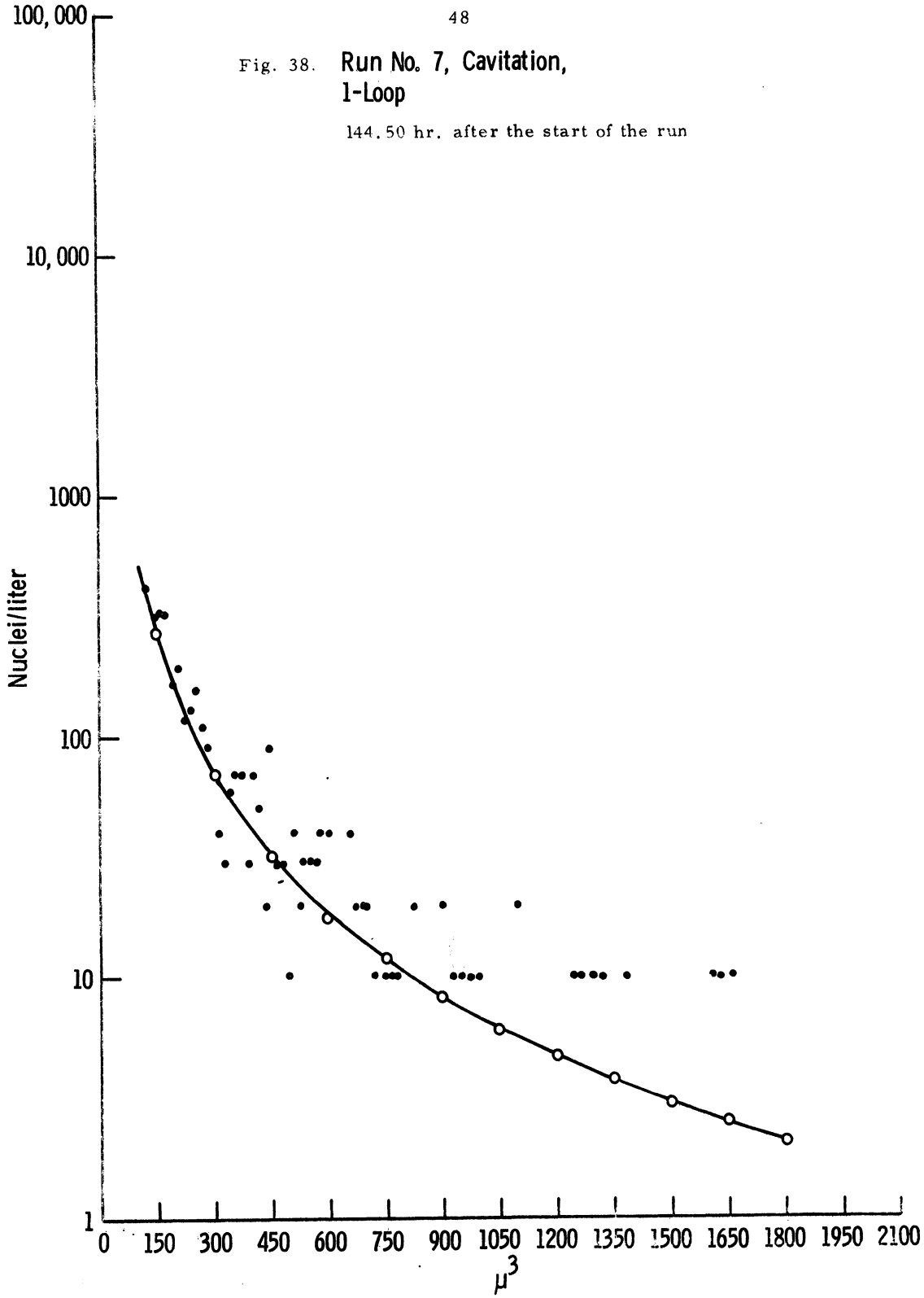

Fig. 39. **Run No. 8, Cavitation, 1-Loop**

167.50 hr. after the start of the run

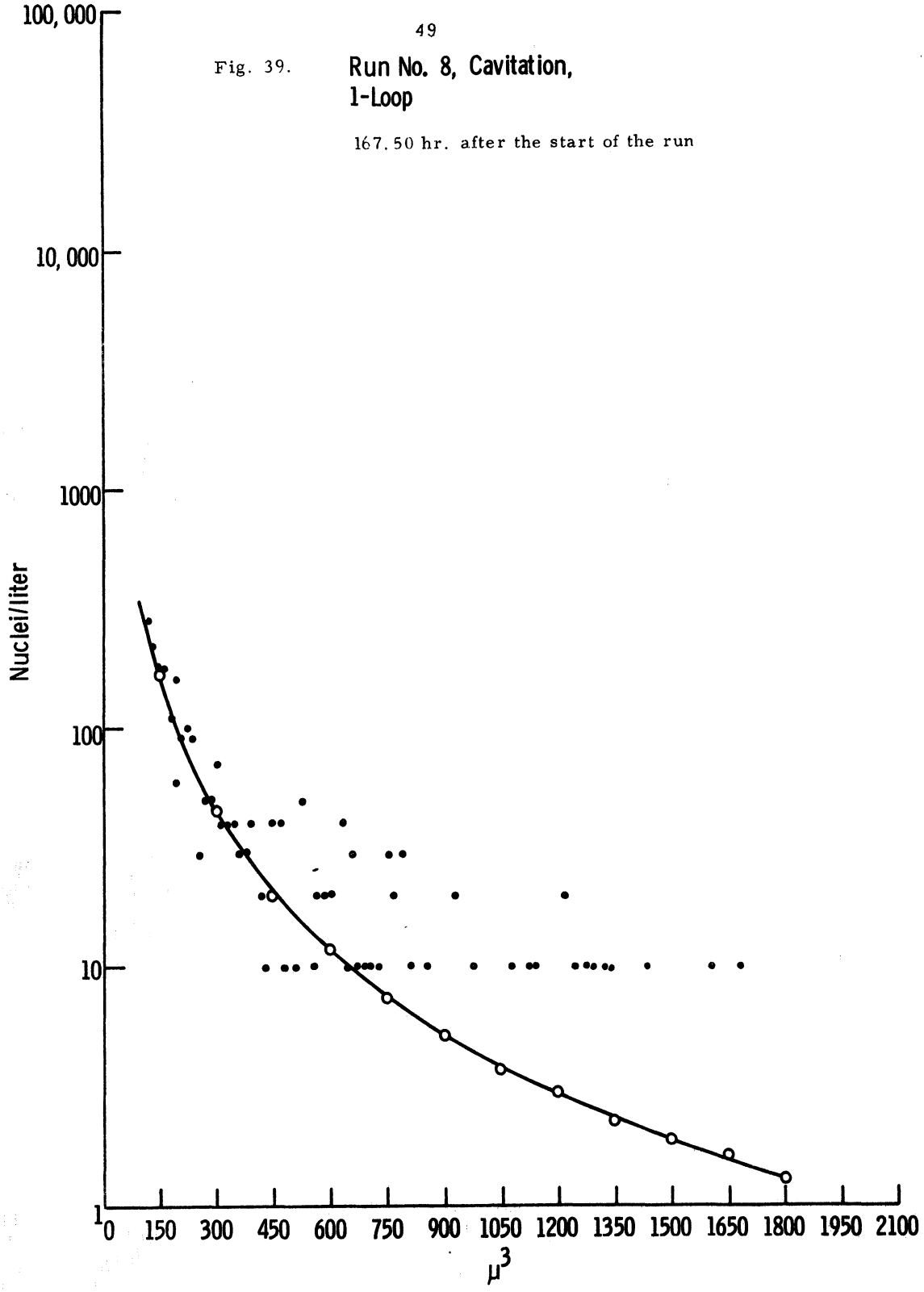

Fig. 40. **Run No. 9, Cavitation, 1-Loop**

191.50 hr. after the start of the run

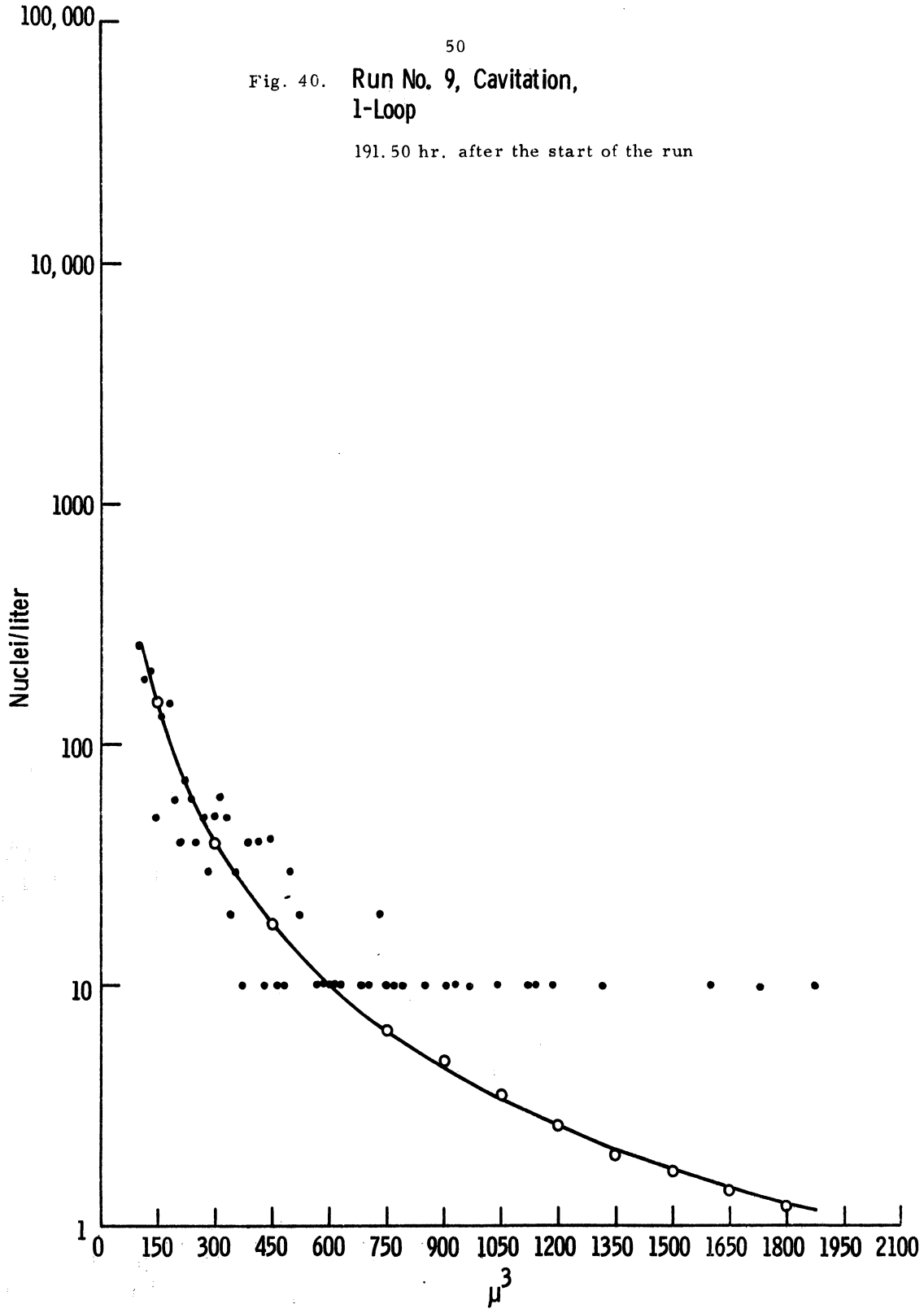

Fig. 41. **Run No. 10, Cavitation, 1-Loop**

220.50 hr. after the start of the run

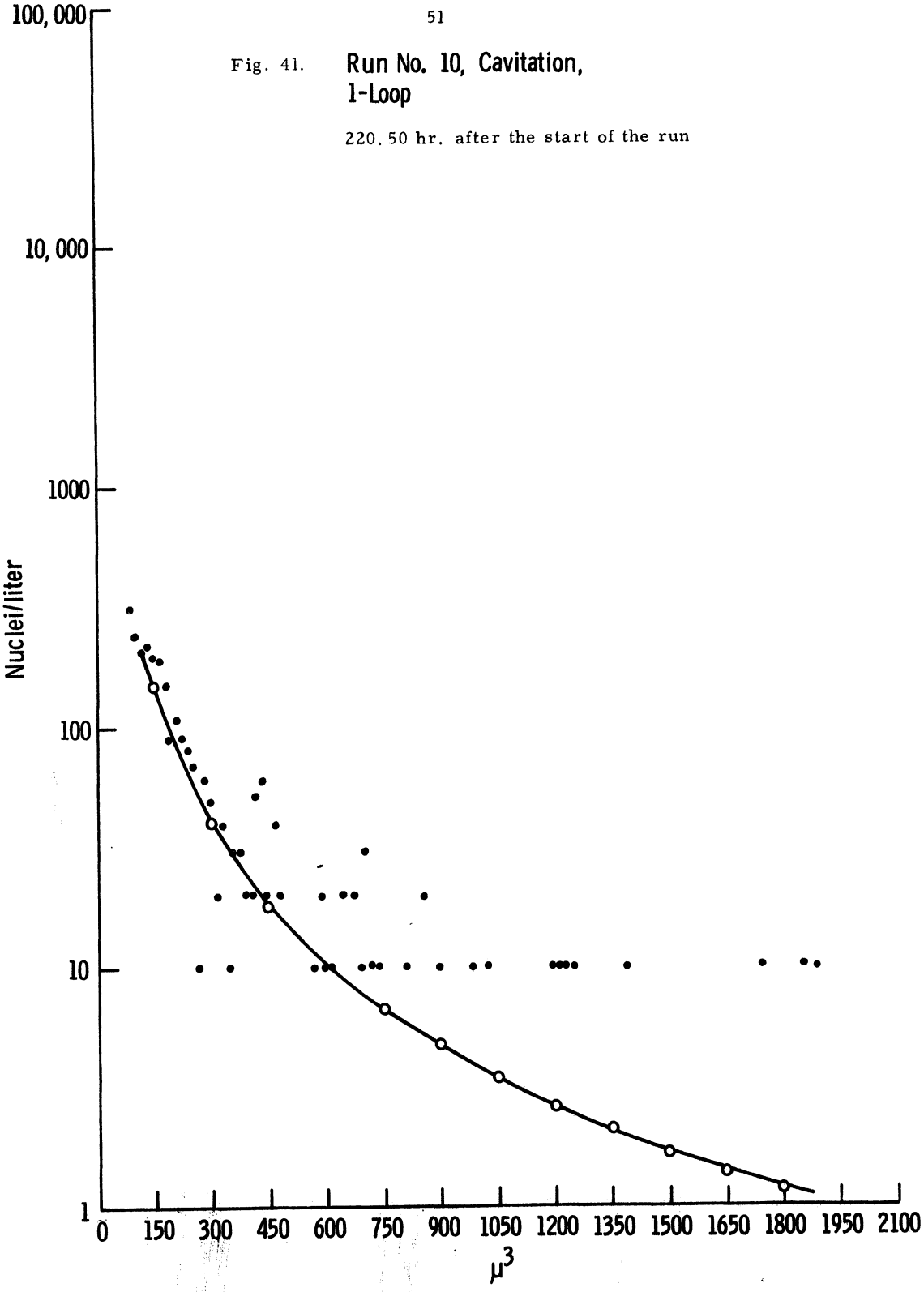

Fig. 42. **Run No. 11, Cavitation, 1-Loop**

246.50 hr. after the start of the run

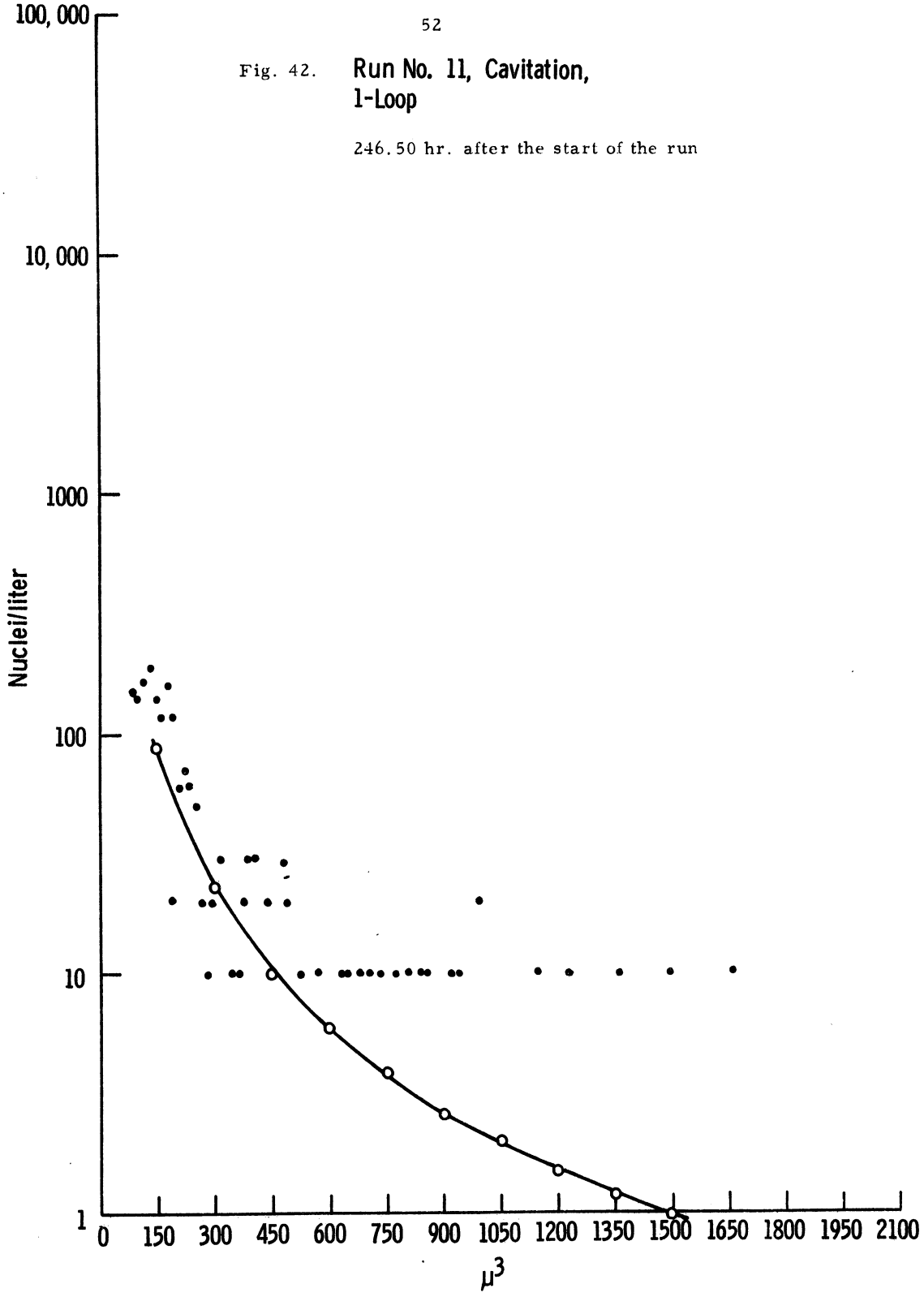

Fig. 43. **Run No. 12, Cavitation, 1-Loop**

265.50 hr. after the start of the run

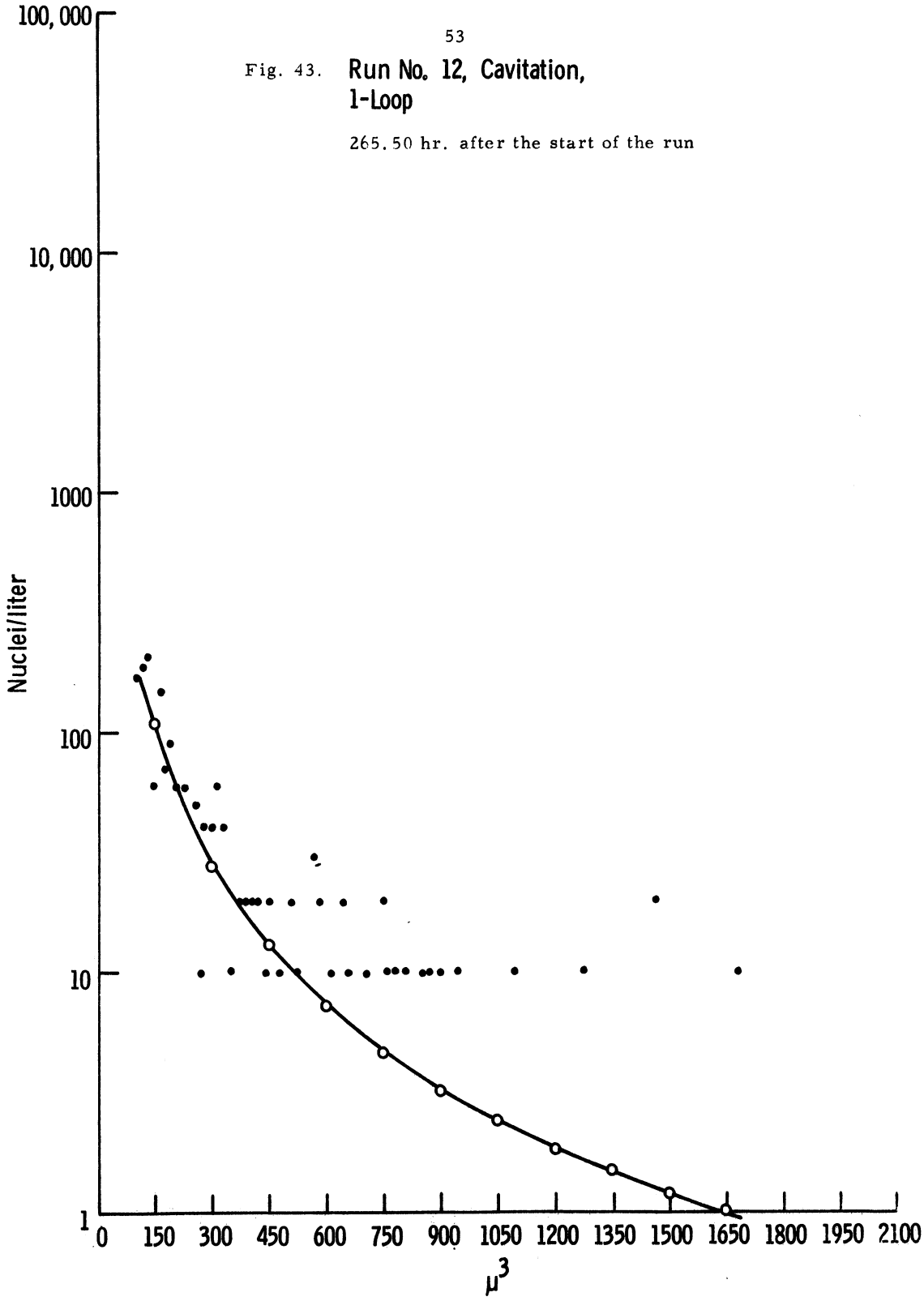

Fig. 44. **Run No. 13, Cavitation, 1-Loop**

289.50 hr. after the start of the run

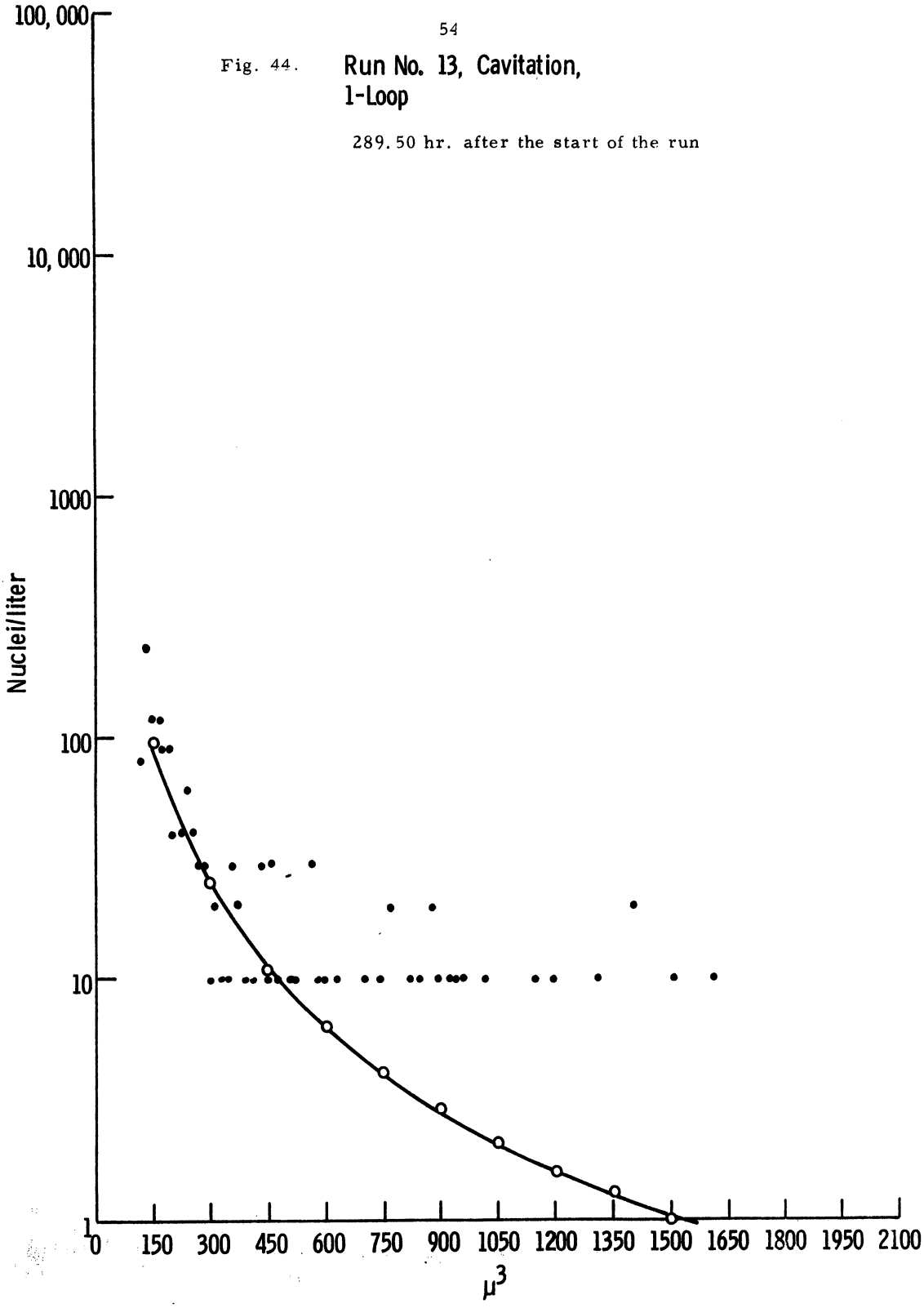

Fig. 45. Run No. 14, Cavitation, 1-Loop

312.50 hr. after the start of the run

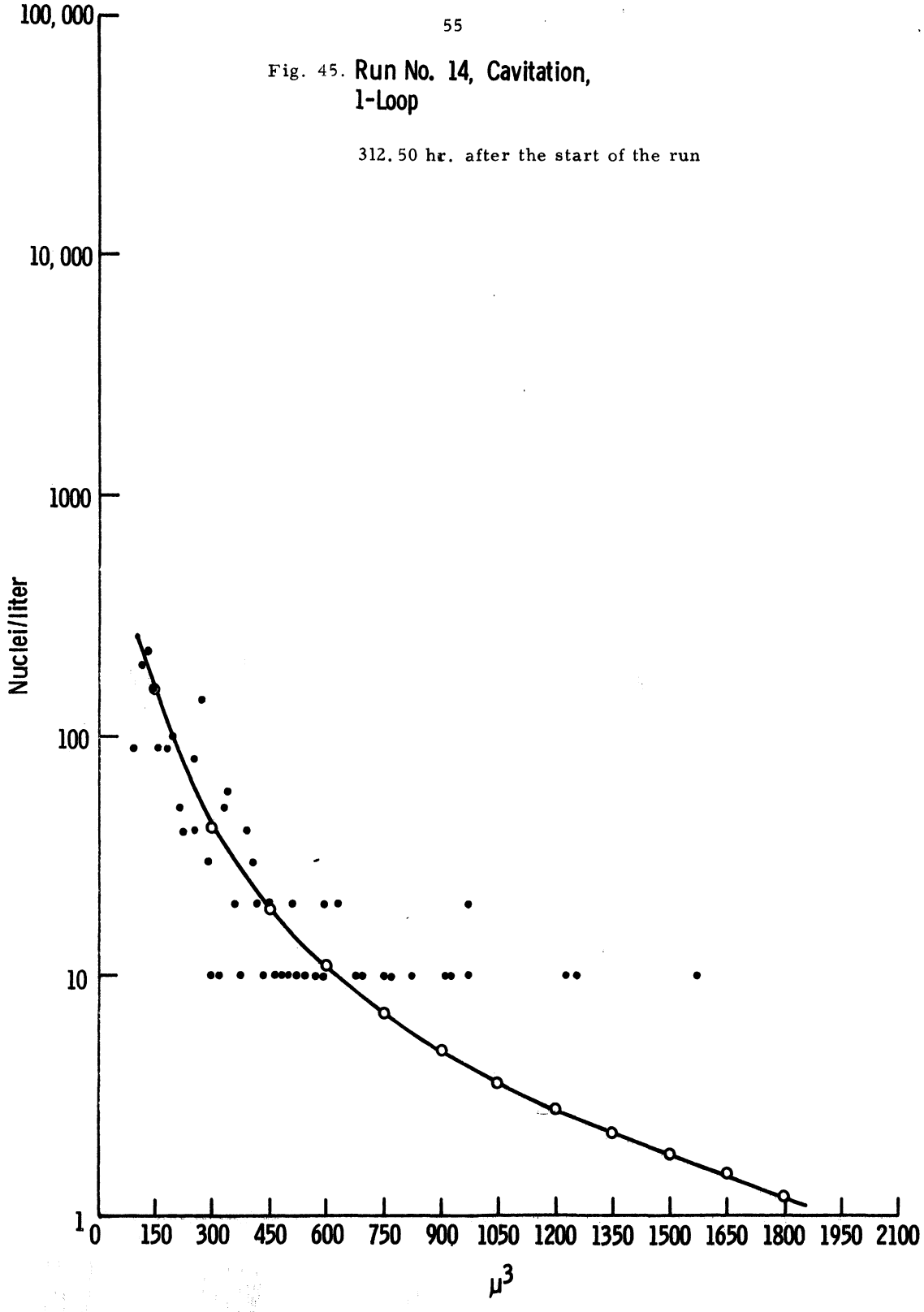

Fig. 46. **Run No. 15, Cavitation, 1-Loop**

337.50 hr. after the start of the run

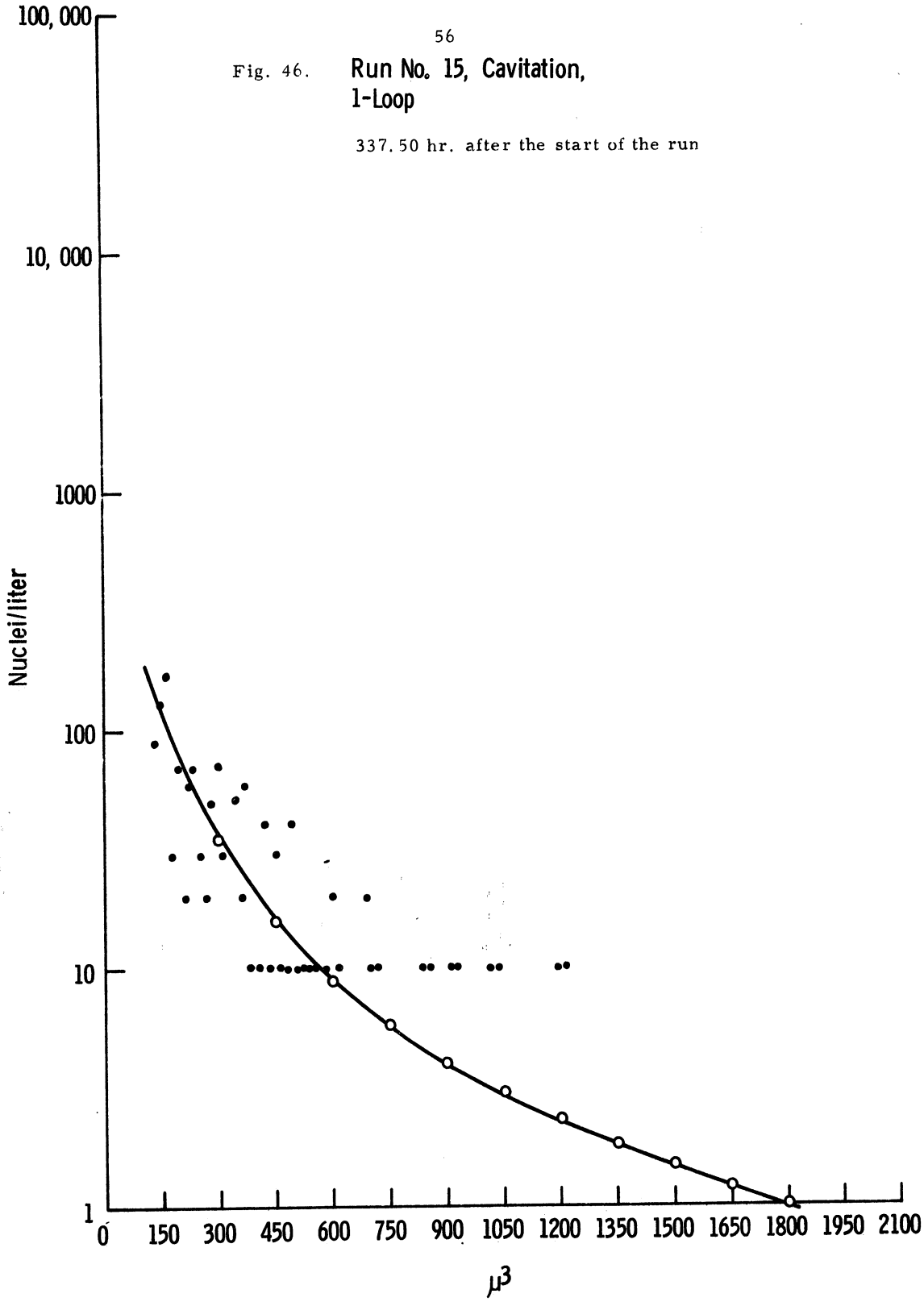

Fig. 47. Cavitation Runs No. 1 through No. 15
1-Loop

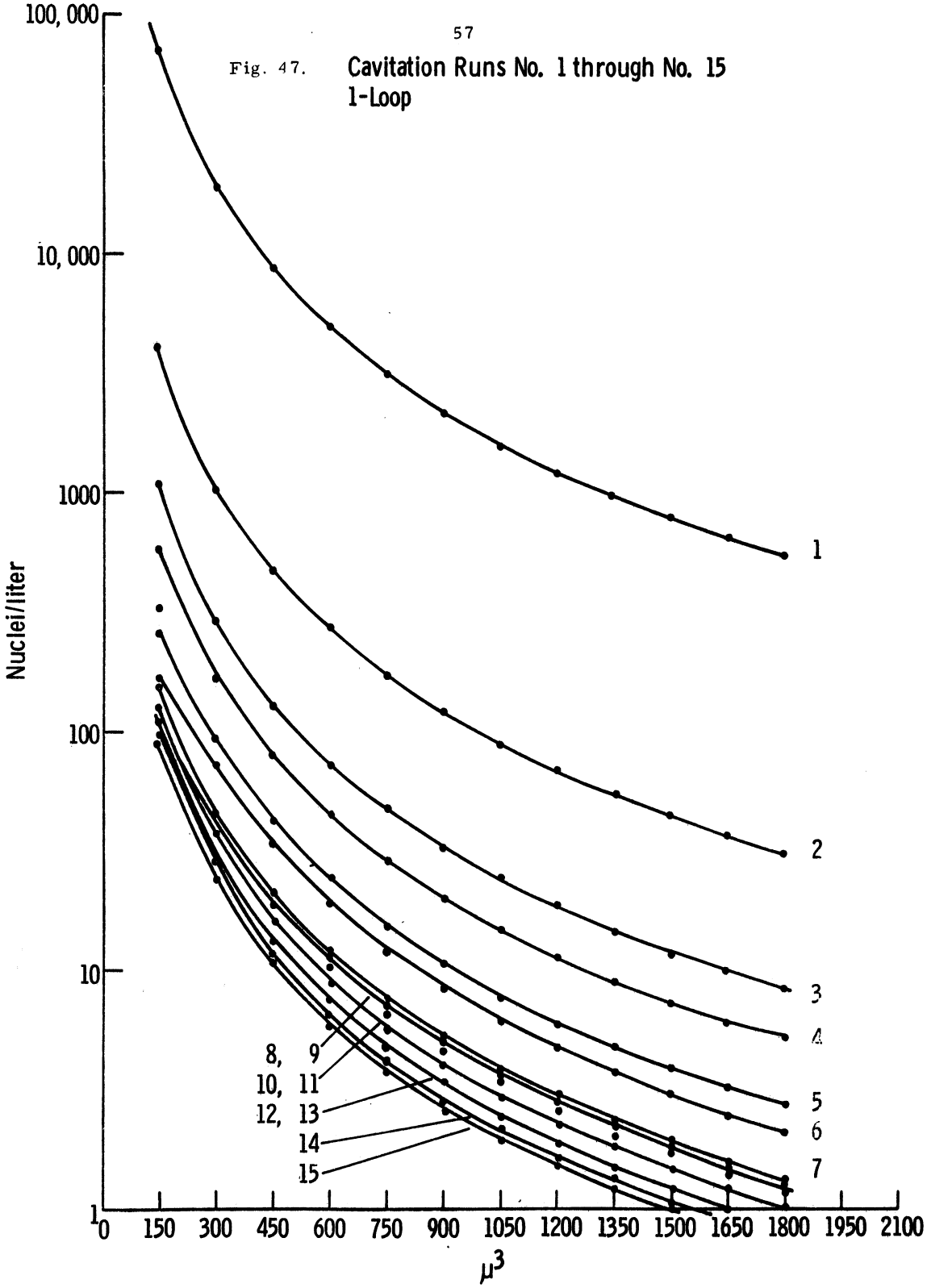

Fig. 48 Entrained gas volume, normalized